How Does an Onion-like Topology Aid in Particle Identification?

Case study: ATLAS detector

Darius CHIȚU
George CHITA

So… why DO they look like ONIONS?

Each particle has a different charge (+/-/0) and extremely different energy intervals. Consequently, each particle deposits its energy at a different radius relative to the beam axis (line) and is stopped by different density materials.

Therefore, a cylindrical design is needed. Detectors, specialized in sensing one specific category of particles, are placed at optimal radii from the beam axis, so that particles stop and deposit most of their energy in those layers, making them easier to be detected. The order in which these layers are constructed is such that each particle signature and calculated parameters are unique.

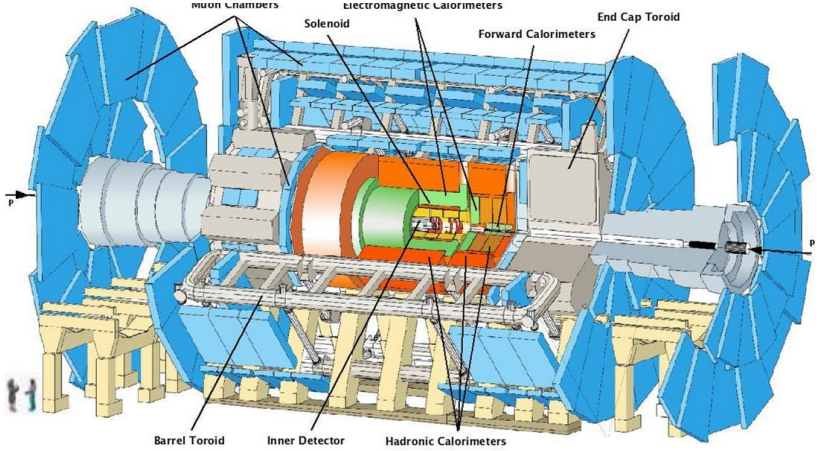

Topology of Particle Detectors

Layers of ATLAS Particle Detector

As we have seen before the ATLAS particle detector consists of several sensor layers divided in two categories, with different functions:

-**Tracking sensors** (measure particle trajectory)

-Pixel Detector (layer 1)

-SCT (semiconductor tracker) (layer 2)

-TRT (transition radiation tracker) (layer 3)

-**Calorimeters** (measure particle energy and momentum)

-LAr Electromagnetic Calorimeter (layer 4)

-Tile Calorimeters (layer 5)

-Muon Spectrometer (layer 6)

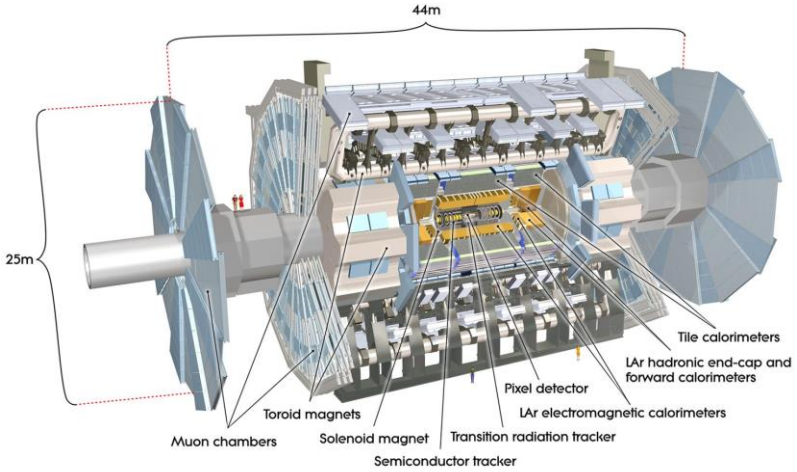

Coordinate System of ATLAS Detector

The ATLAS particle detection system makes use of 6 coordinates, of which, for the purpose of this presentation, we will only be interested in Φ,R and z which respectively correspond to azimuth, radius and distance from the center point (point of collision).

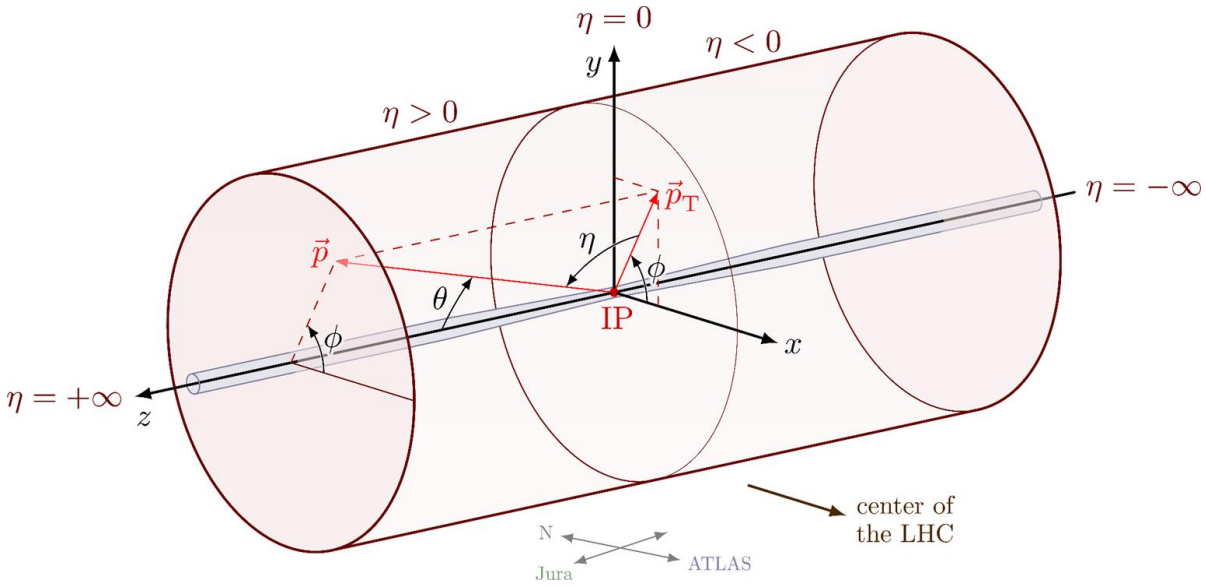

Pixel Detector

The pixel detector represents the innermost layer of the ATLAS detector. It is mainly comprised of rectangular modules, each 62.4x22.4 mm, containing 61440 (for each module) individual microscopic pixels. The modules are arranged in 3 layer as follows:

Layer 1 PD - R=50.5 mm, 22 modules
Layer 2 PD - R=88.5 mm, 32 modules
Layer 3 PD - R=122.5 mm, 52 modules

There is a 20° angle between any two neighbouring modules.

It gives R,Φ and z coordinates.

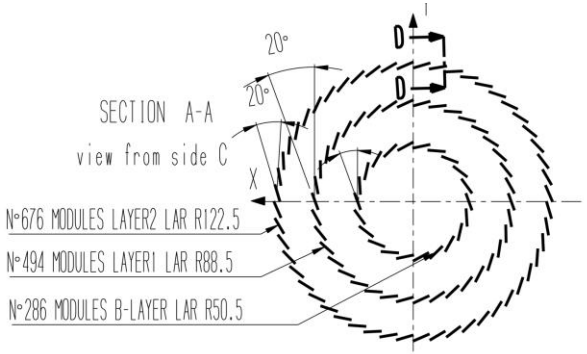

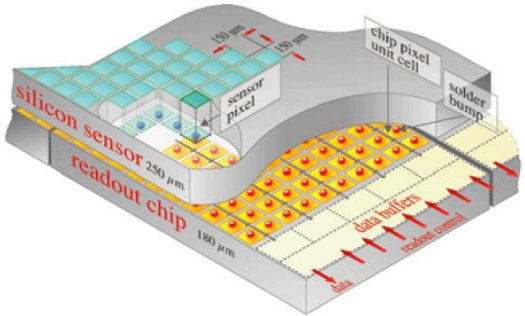

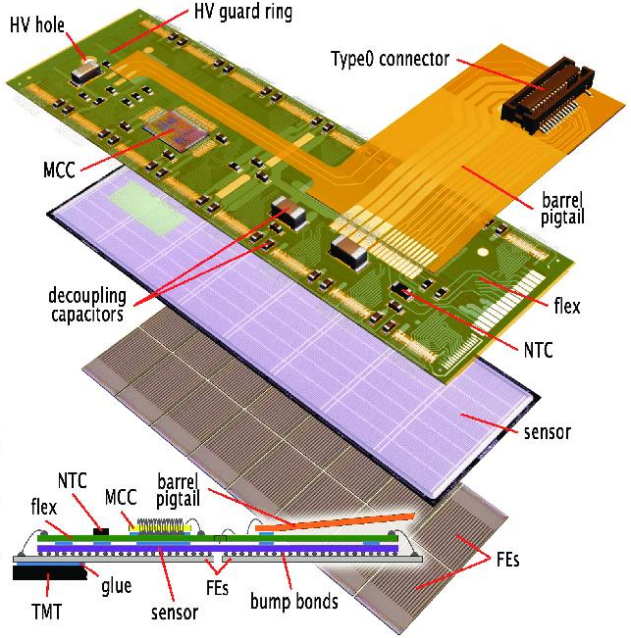

How Does the Pixel Detector Work?

For each pixel, a silicon wafer doped with p and n type semiconductors is used.

Quick explanation:

-p doping means introducing a boron impurity into the crystal lattice of silicon atoms. These boron atoms are missing an electron relative to the silicon. These so called “holes” imitate the existence of a free positive charge carrier.

-n doping means introducing a phosphorus impurity to the crystal lattice which carries with it an extra electron. This extra electron acts like a negative free charge carrier.

In a semiconductor, a depletion layer is formed at the junction between these two materials.
What is a depletion layer?

Keep in mind that the material is electrically neutral from a global point of view, as the number of protons in the nucleus is equal to the number of electrons around it, for all three elements. Still, a positive “hole”, from the p-type gets attracted to the electrons in the n-type as its position is more favorable there. Vice-versa for electrons in n-type. The particles migrate until the electric force (created by their electric field) is equal to their attraction to the opposite side. (Usually 0.7V for silicon)

How Does the Pixel Detector Work?

This is the basic working principle of a diode. If a voltage is applied that creates an electric field in the direction of the depletion region electric field, the depletion region will grow until the voltage potential of the layer will be equal and opposite to the potential that is applied, and no current will flow. Still, this is a conductor, so when a particle hits and knocks off some electrons from the atoms, a current will flow to replace those electrons. This current can be easily measured and analyzed further. The ingenuity of this design is that even though the detector is a conductor, it doesn't allow current to pass until a particle is detected.

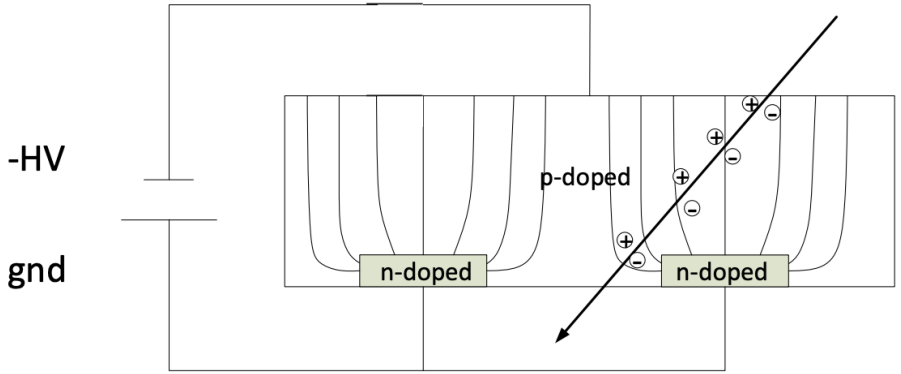

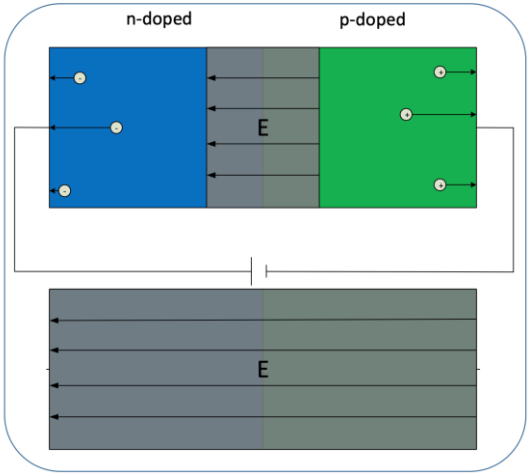

Semiconductor Tracker

The semiconductor tracker is the 2’nd major layer of the ATLAS detector, comprised of sublayers 4,5 and 6, each consisting of detector sensors sized 63.4x64 mm. Each of the sensors consists of 768 silicon strips spaced out equally, with a pitch of 80um.

One module contains two sensors daisy-chained back to back, with a total length of 128mm.

To ensure that all particles cross at least one module, the main detector barrel, has several circular end caps built with different trapezoidal sensors, but having the same working principle.

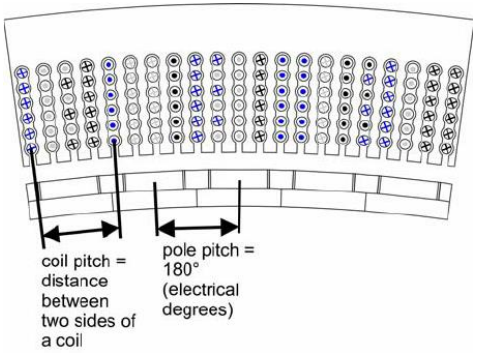

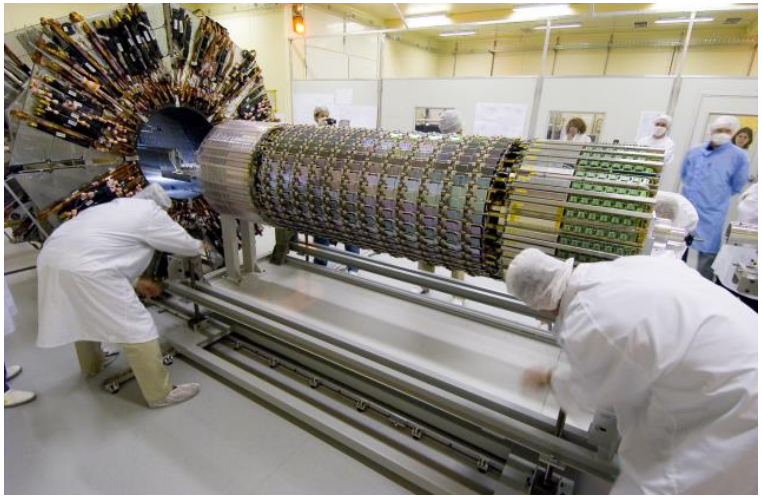

It gives R,Φ coordinates.

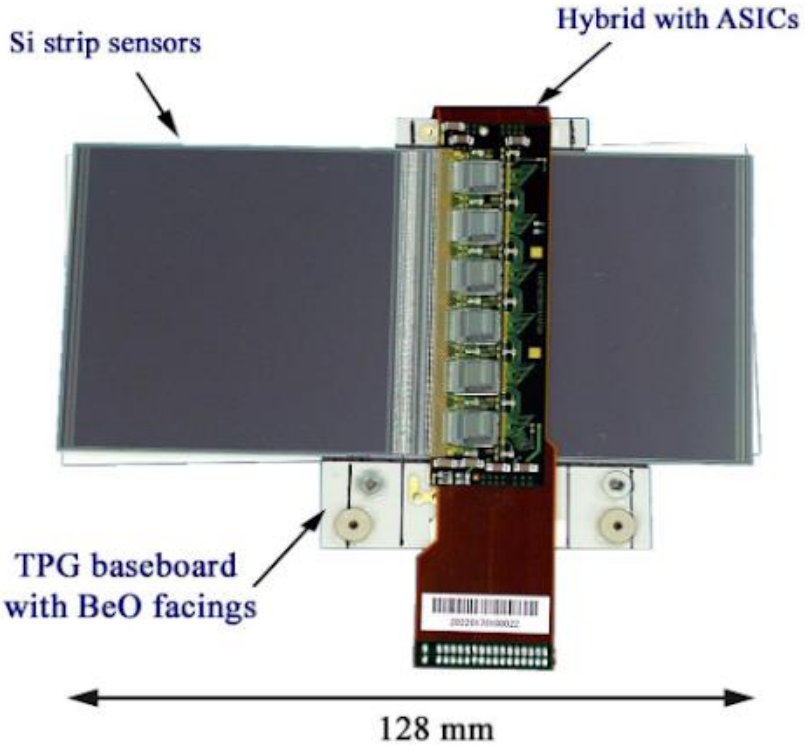
Si strip sensors
Hybrid with ASICs
TPG baseboard
with BeO facings
128 mm

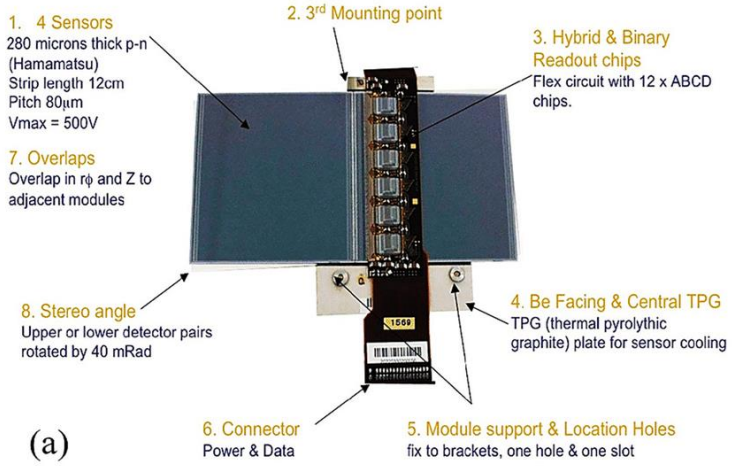
1. 4 Sensors
280 microns thick p-n
(Hamamatsu)
Strip length 12cm
Pitch 80μm
Vmax = 500V
2. 3rd Mounting point
3. Hybrid & Binary
Readout chips
Flex circuit with 12 x ABCD
chips.
7. Overlaps
Overlap in rφ and Z to
adjacent modules
8. Stereo angle
Upper or lower detector pairs
rotated by 40 mRad
4. Be Facing & Central TPG
TPG (thermal pyrolythic
graphite) plate for sensor cooling
6. Connector
Power & Data
5. Module support & Location Holes
fix to brackets, one hole & one slot
(a)

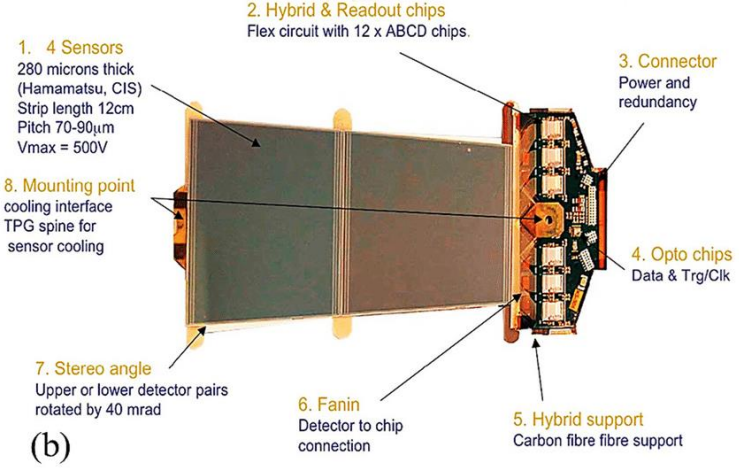
2. Hybrid & Readout chips
Flex circuit with 12 x ABCD chips.
1. 4 Sensors
280 microns thick
(Hamamatsu, CIS)
Strip length 12cm
Pitch 70-90μm
Vmax = 500V
3. Connector
Power and
redundancy
8. Mounting point
cooling interface
TPG spine for
sensor cooling
4. Opto chips
Data & Trg/Clk
7. Stereo angle
Upper or lower detector pairs
rotated by 40 mrad
6. Fanin
Detector to chip
connection
5. Hybrid support
Carbon fibre fibre support
(b)

How does a SCT sensor work?

Huaraaayyy! No more boring explanations!

It works exactly the same as the pixel detector, except that the sensors are strips, and the p-type is inside the n-type conductor. **Here is a cat for your relaxation:**

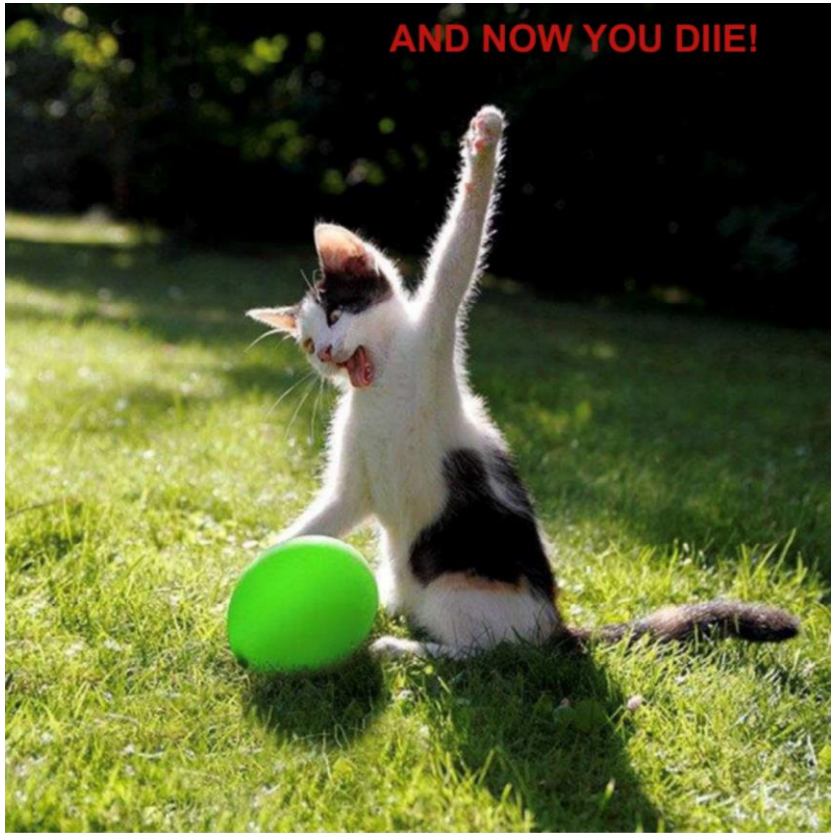

Transition Radiation Tracker

The TRT is based on the use of parallel metal straws, each 1440 mm long (along the beam axis), with a thin gold-plated tungsten wire at the middle, surrounded by a mixture of gases (70% Xe 27% CO2 3%O2). There are 96 trapezoidal modules, which in total contain about 50,000 parallel straws, and, as we have seen in the case of the SCT, the TRT also makes use circular end caps comprised primarily of 320,000 radial straws starting from an inner radius of 640 mm to an outer radius of 1040mm, with the exception of the last four caps, which have an inner radius of 480mm (overlapping with the SCT endcaps and not allowing any particles to escape). In total the TRT has 420,000 readout channels, as each straw is divided in half and only has one output cable.

It gives R,Φ coordinates.

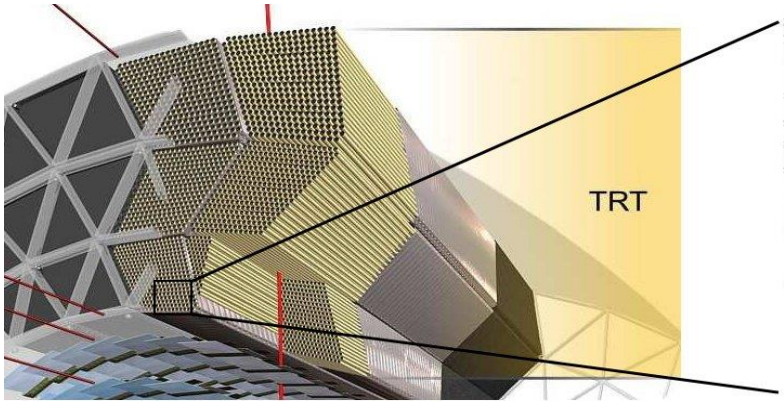

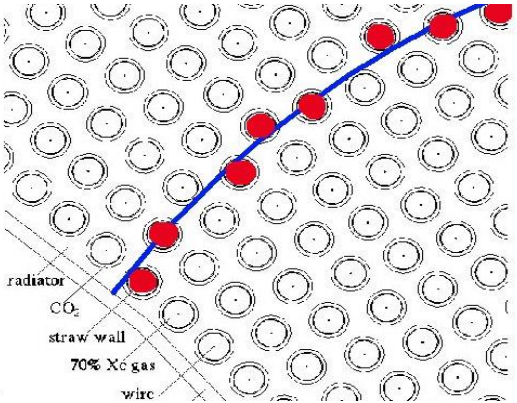

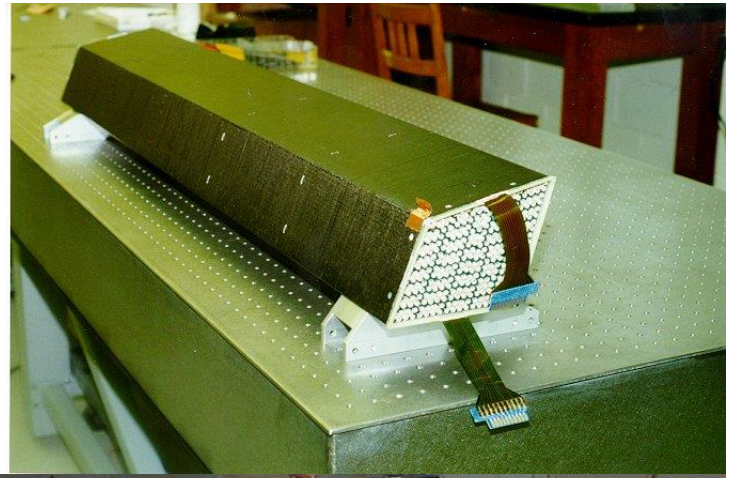

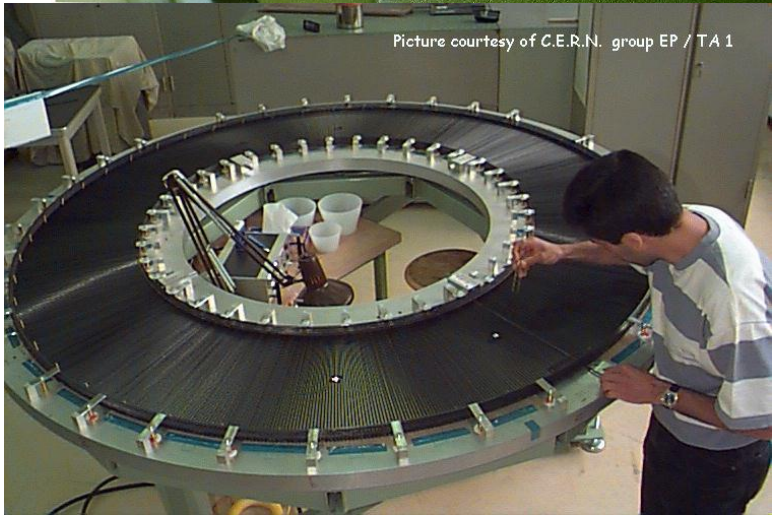
Picture courtesy of C.E.R.N. group EP / TA 1

How does a TRT detector work?

In simple terms, an energetic particle that passes through the detector ionizes, a combination of gases inside of the straws (70% Xe; 27% CO2; 3%O2), creating charge carriers (gas ions and free electrons) that get attracted and deposit their charge on the different electrodes (outer pipe, and inner wire) outputting an electrical pulse. This is very similar to how all basic geiger tubes work.

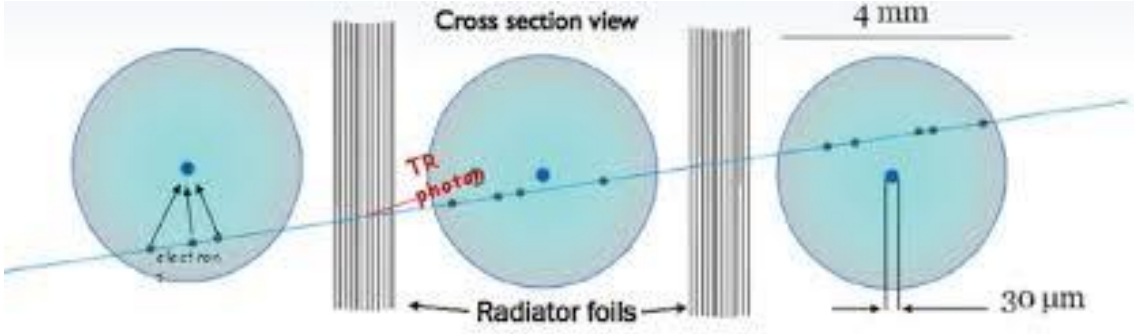

Liquid Argon Electromagnetic Calorimeter

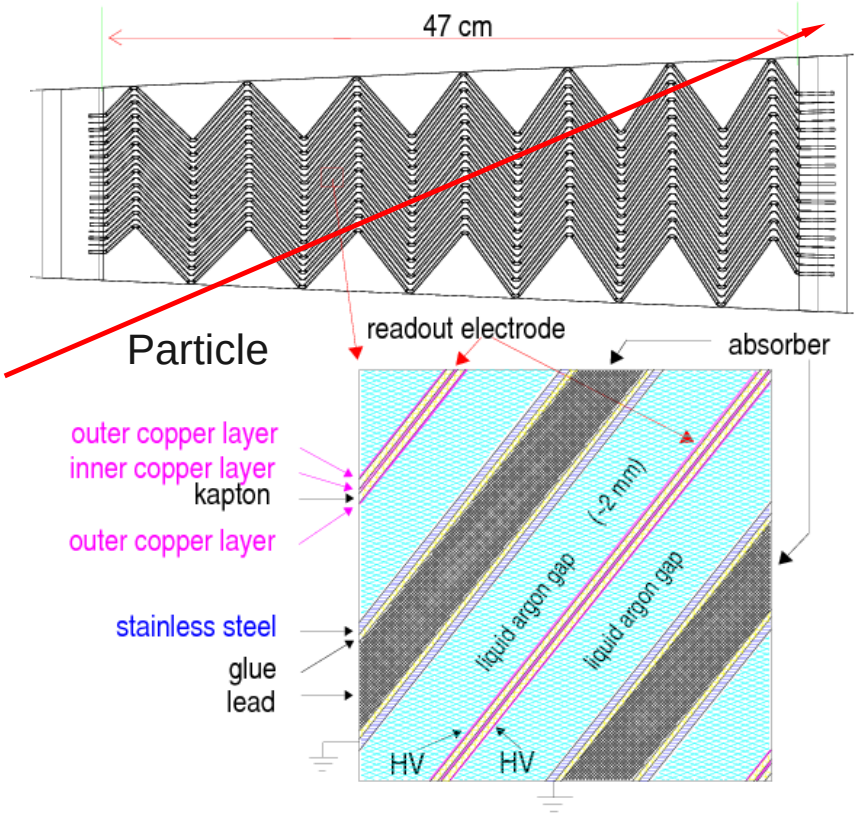

The LAr electromagnetic calorimeter consists of several layers of copper coated in a thin layer of lead in between layers of readout copper electrodes held at a high voltage potential. In between these two layers, sits a 2 mm thick layer of liquid argon at a temperature of about -186°C. The layers of lead plated copper are bent in a zig-zag pattern (with sides of 43.76mm), such that the tight angles do not permit the passing of a particle without it depositing its energy in one of the layers. The central barrel of the calorimeter is 6.4 m long and with 53 cm thick walls.

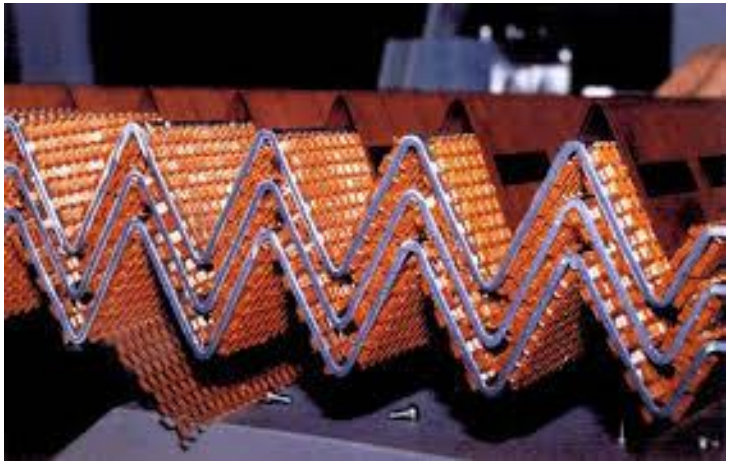

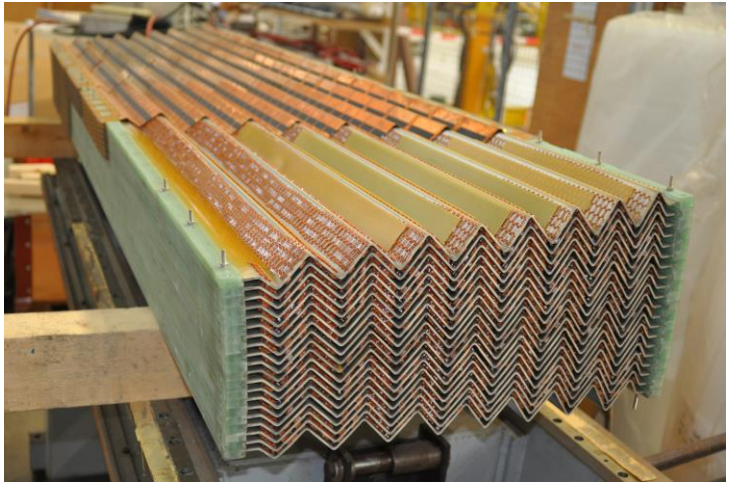

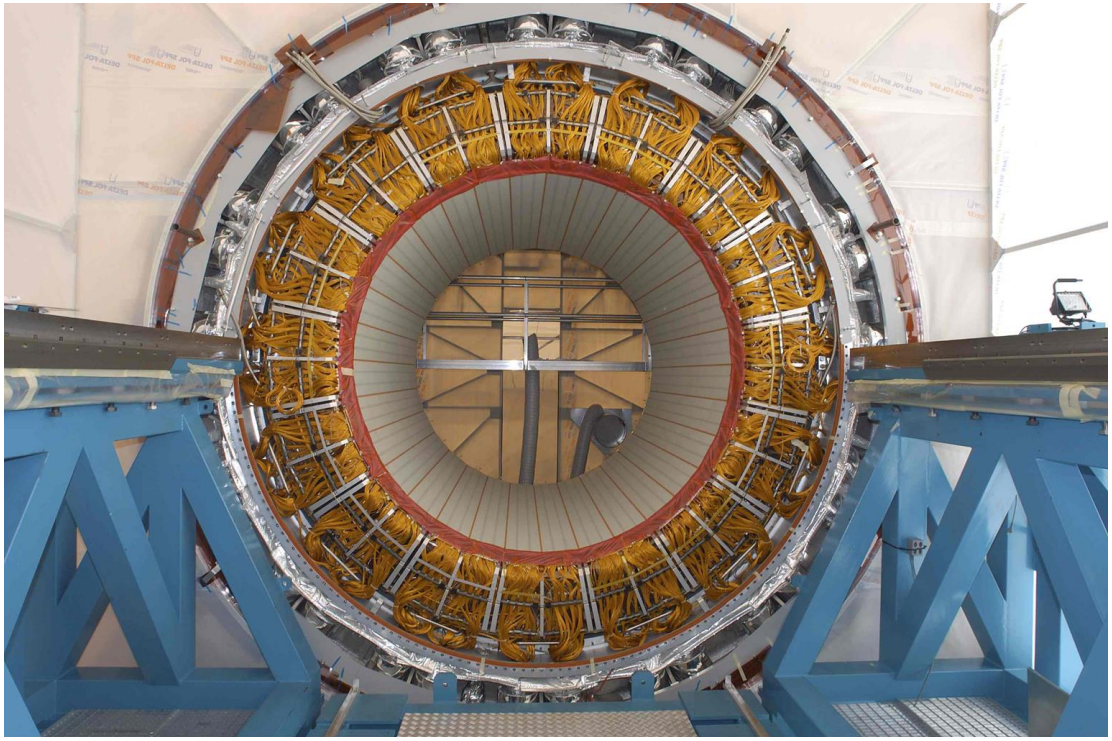

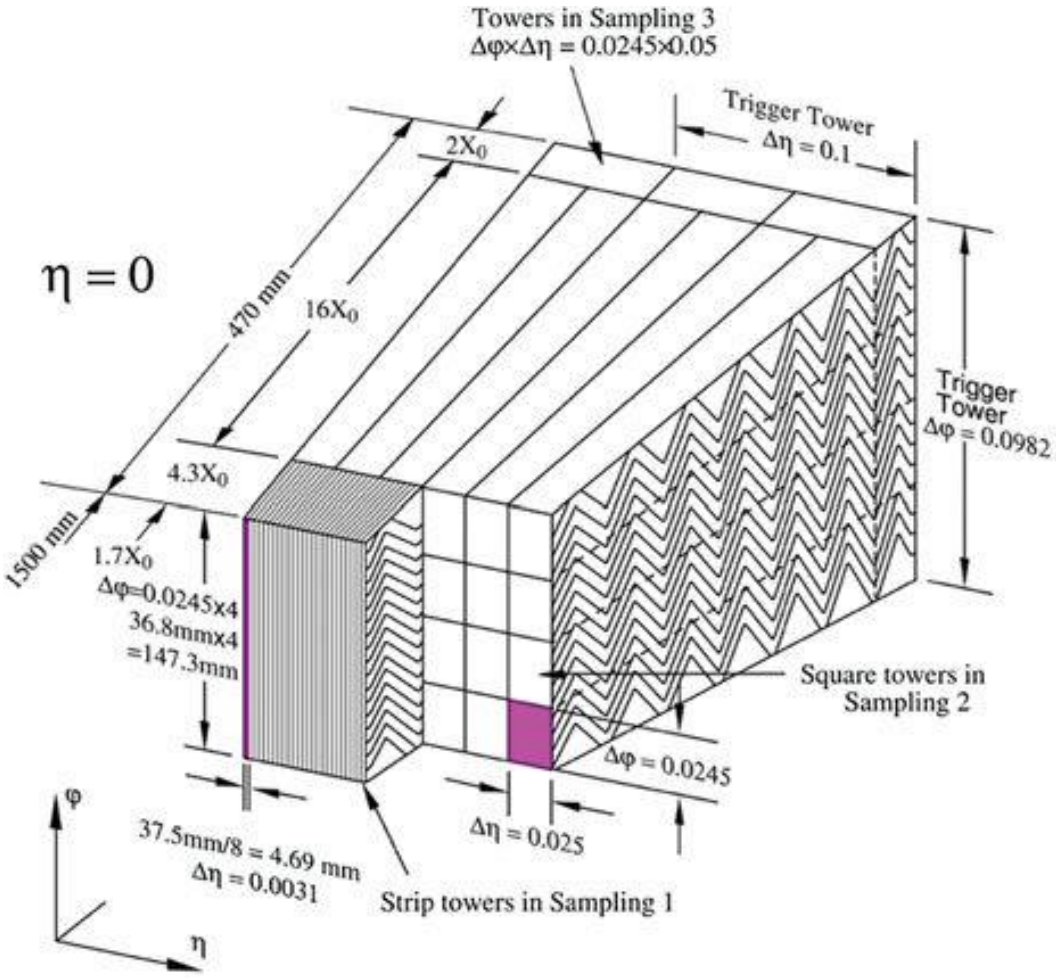
Towers in Sampling 3
Δφ×Δη = 0.0245×0.05
Trigger Tower
Δη = 0.1
2X0
η = 0
470 mm
16X0
Trigger
Tower
Δφ = 0.0982
4.3X0
1500 mm
1.7X0
Δφ=0.0245x4
36.8mmx4
=147.3mm
Square towers in
Sampling 2
Δφ = 0.0245
φ
37.5mm/8 = 4.69 mm
Δη = 0.0031
Δη = 0.025
Strip towers in Sampling 1
η

How does the LAr Electromagnetic Calorimeter Work?

When a particle passes through the different layers of the detector it ionizes the argon atoms and creates freely moving charge carriers that get attracted to the anode/cathode where they deposit their charge and create an electrical signal.(In other words it creates a slightly conductive path) The voltage difference between the different detector layers is around 2000V. Argon is optimal as it has a very low ionization energy of just 26eV per atom, per first electron.

Tile Calorimeter

The tile calorimeter is comprised of 64 modules per a 360° slice, each covering an angle of approximately 5.62°, starting from an inner radius of 2280mm to an outer radius of 4230m.

A module consists of 576 alternating iron plates sandwiched between a scintillator 3 mm thick polymeric material (polystyrene), with a ratio of iron to scintillator of 4.7 to 1. There are 11 such layers on top of each other, shifted by a slight amount. The photons can reach the multiplier ,even if the layers of iron are shifted and there is no free path to the tube, by means of WLS fibers. (The ends are silver coated as not to allow light to escape)

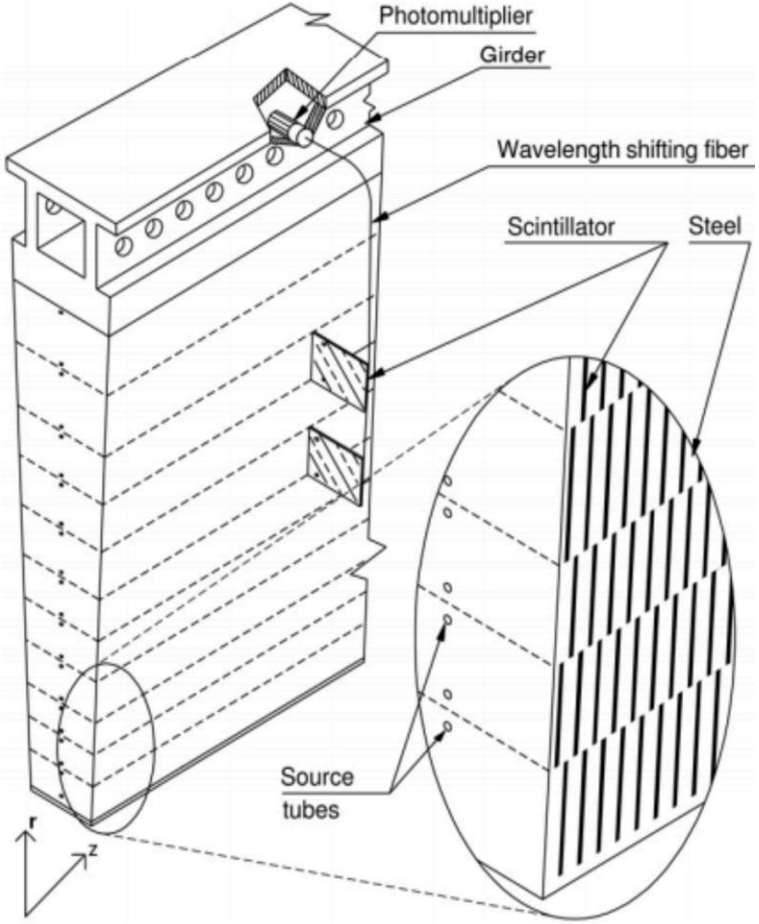

Quick explanation of what WLS fibers are (wavelength shifting)

Wave-Length Shifting (WLS) optical fibers are used to collect the light produced in the scintillator tiles. The plastic in these fibers have been doped with special dyes that absorb the predominantly blue photons from the scintillator and re-emit even more green ones, allowing the PMT to better detect the particles.

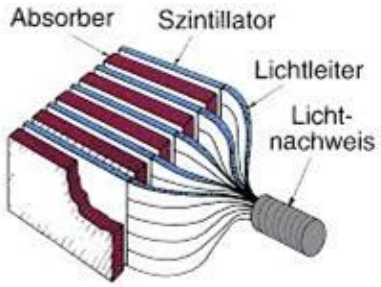

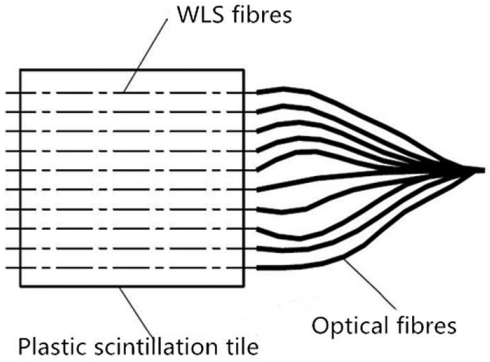

Description	Emission			Absorption Peak[nm]	Att.Leng.[2] [m]	Characteristics
	Color	Spectra	Peak[nm]			
Y-7(100)	green	See the following figure	490	439	>2.8	Blue to Green Shifter
Y-8(100)	green		511	455	>3.0	Blue to Green Shifter
Y-11(200)	green		476	430	>3.5	Blue to Green Shifter (K-27 formulation) Long Attenuation Length and High Light Yield
B-2(200)	blue		437	375	>3.5	UV to Blue shifter
B-3(200)	blue		450	351	>4.0	UV to Blue shifter
O-2(100)	orange		550	535	>1.5	Green to orange shifter
R-3(100)	red		610	577	>2.0	Green to red shifter

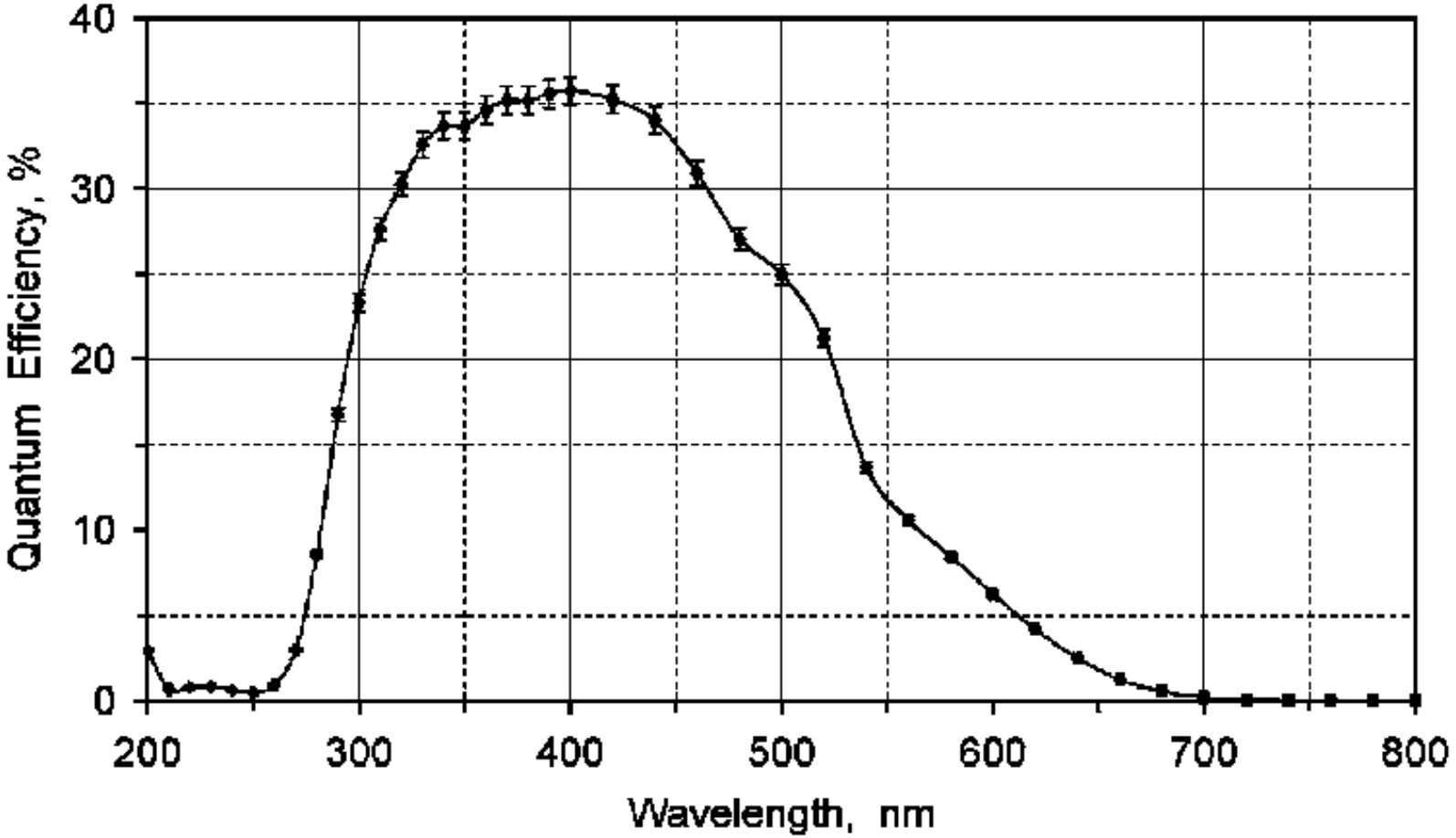
Quantum Efficiency, %
0
10
20
30
40
200
300
400
500
600
700
800
Wavelength, nm


[5]

Tile Calorimeter

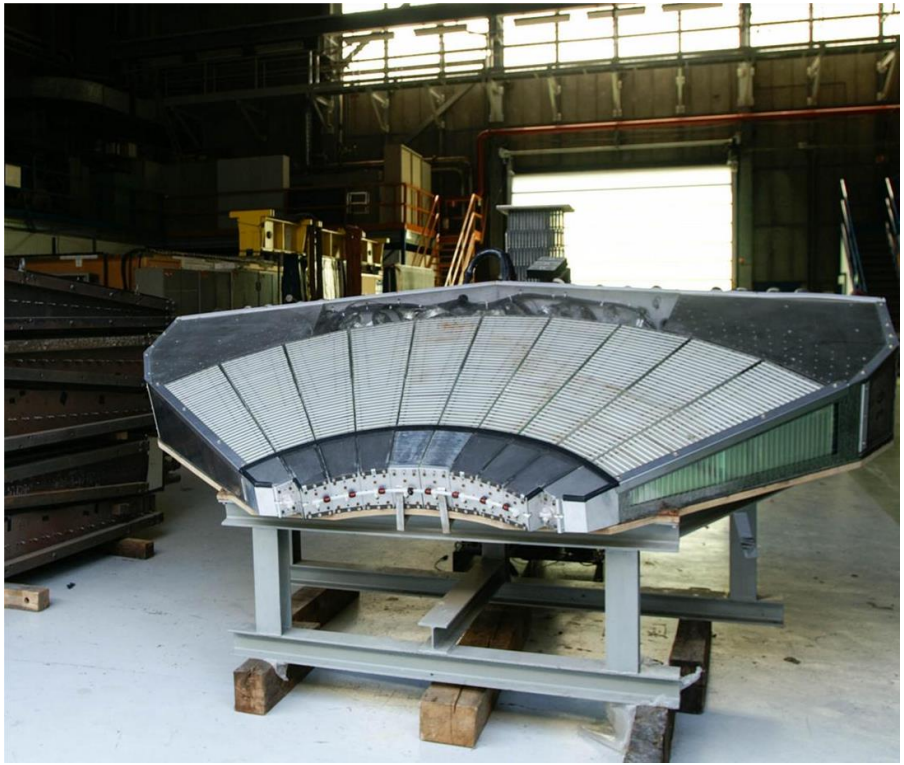

The plane of the scintillator and iron plates is parallel to the plane of the beam axis, in order to allow incoming particles to pass in between these layers, and not intersect them directly, which would slow down the particles much quicker. At the end of each module sits a photomultiplier tube, which transforms the incoming photons into a stronger electrical pulse, that then gets amplified and analyzed. The topmost layer has a width of 369mm while the bottom one is only 231mm and a radial height ranging from 97 to 187mm (from bottom to top).

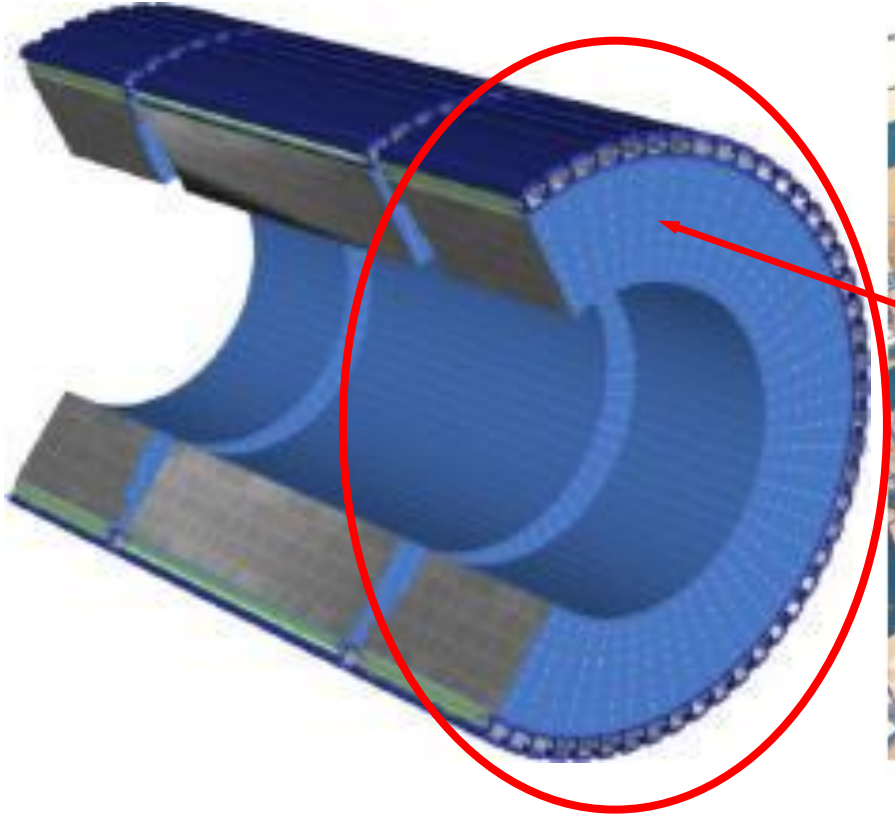

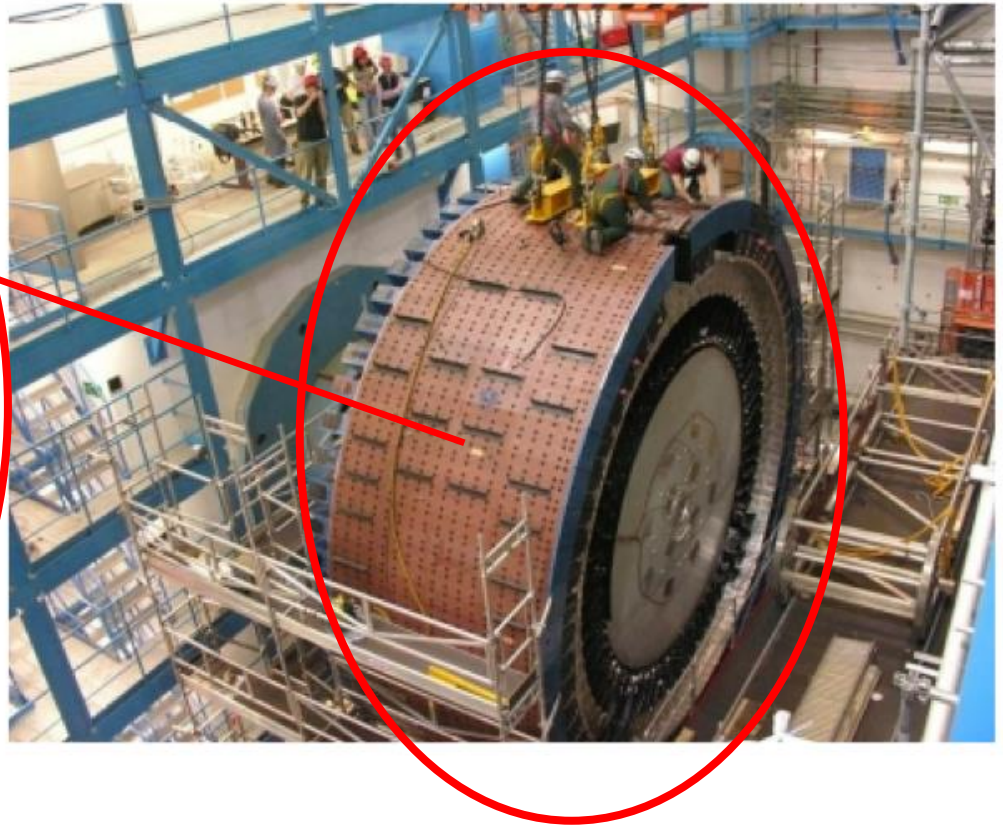

How do Scintillators Work?

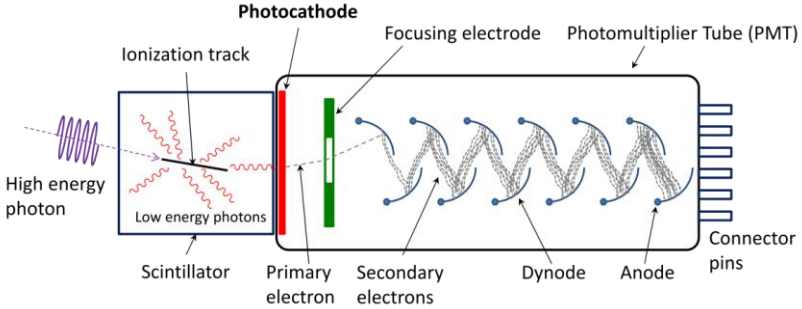

When a high energy photon hits an electron in the region of a nucleus, the electron absorbs the photon's energy and gets raised to a higher energy level. After a short amount of time, the electron starts re-emitting lower energy photons until it drops down to the energy level it started from. Quantization of energy (Bohr's postulate). The combined energy of the re-emitted photons equals the initial energy, so energy is conserved.

The photons emitted get directed into the PMT and get amplified.

How does a Photomultiplier Tube Work? (In general-Not ATLAS)

The photomultiplier tube consists of multiple photo-emitting cathodes, held at a voltage difference of about 100V from each other, in a very good vacuum (10uPa). When a photon strikes the first cathode, via the photoelectric effect, it emits a few electrons that get accelerated to the neighbouring cathode, where the process repeats, and, in the end, a strong electrical signal can be measured. This process happens generally with semiconductors (bialkali antimonides) as they have the valence band very close to their conduction band, needing a very low energy to raise an electron into the conduction band.

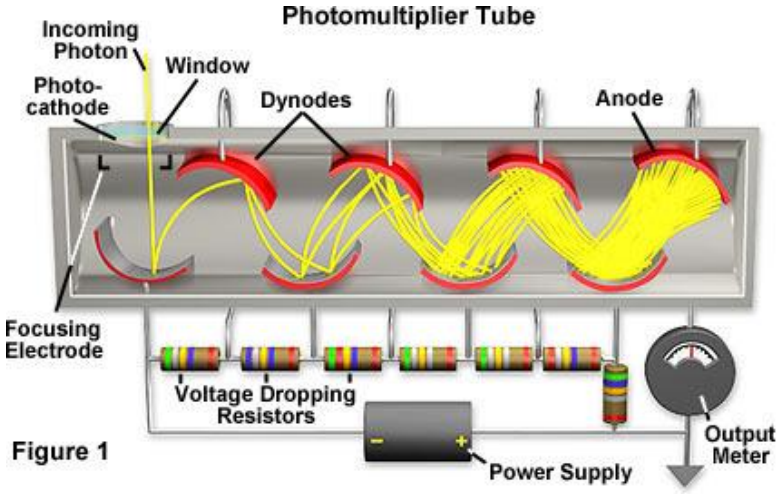

Figure 1

Muon Spectrometer

The muon spectrometer is composed of four different types of detectors: MDT (monitored drift tube), RPC (resistive plate chambers), TGC (thin gap chambers) and CSC (cathode strip chambers).

-Monitored Drift Chambers (MDT) are used in the ATLAS Detector to measure the momentum of high energy muons. They consist of aluminum tubes (3 cm in diameter), which are filled with an Ar-CO2 gas mixture at 3 bar of pressure and additionally contain a thin metal wire at the center (anode). About 1200 drift chambers are required for ATLAS. They are up to 6 m long, and are primarily found in the barrel and end cap region.

-RPCs consist of two parallel plates, a positively-charged anode and a negatively-charged cathode, both made of a very high resistivity plastic material and separated by a thin gas volume, sandwiched between copper strips and thin layer of aluminum foil (charged to a high potential). When a muon passes through the chamber, electrons are knocked out of the atoms of the gas. These electrons in turn hit other atoms causing an avalanche of electrons. The electrodes are transparent to the signal (the electrons), which are instead picked up by external metallic strips after a small but precise time delay. These detectors build up a large section of ATLAS's main barrel.

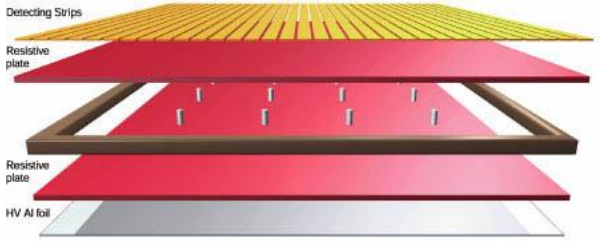

Muon Spectrometer

-Thin gap chambers are made by sandwiching 50um gold plated tungsten wire with a pitch of 1.8 mm at a 1.4 mm distance from a bottom resistive graphite epoxy plate and top copper pads with a pitch of only 80mm. Under the resistive plate there are placed very fine 3.2 mm pitch, plated, copper strips. The chamber is filled with a gas mixture of 55% CO2 and 45% n-pentane to which a 2.9kV/cm electric field is applied (in order to direct ionized particles). The TGC comprise most of the detector's end caps.

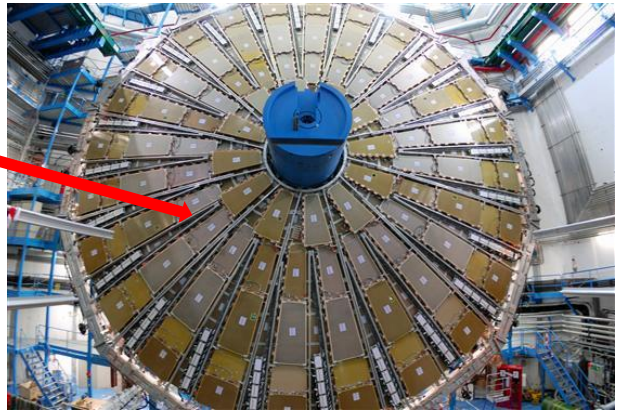

-Cathode strip chambers consist of arrays of positively-charged anode wires crossed with negatively-charged copper cathode strips within a gas volume. When muons pass through, they knock electrons off the gas atoms, which flock to the anode wires creating an avalanche of electrons. Positive ions move away from the wire and towards the copper cathode, also inducing a charge pulse in the strips, at right angles to the wire direction.

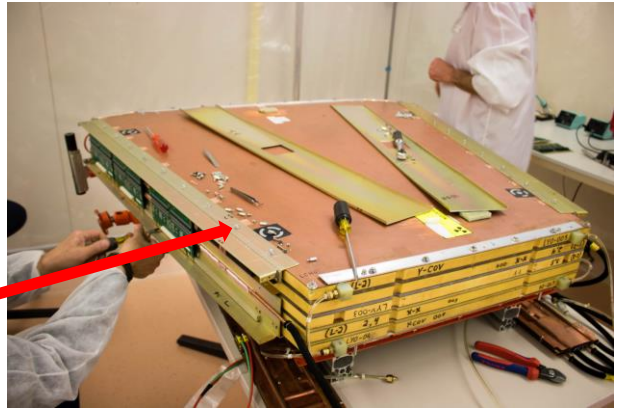

MDT

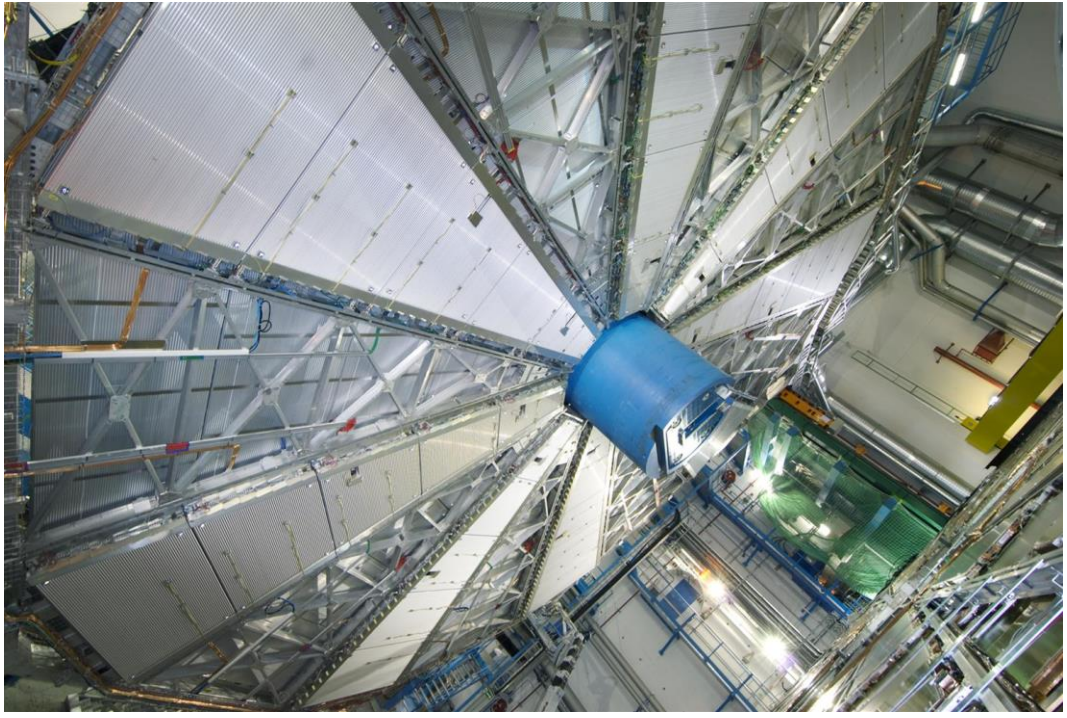

RPC

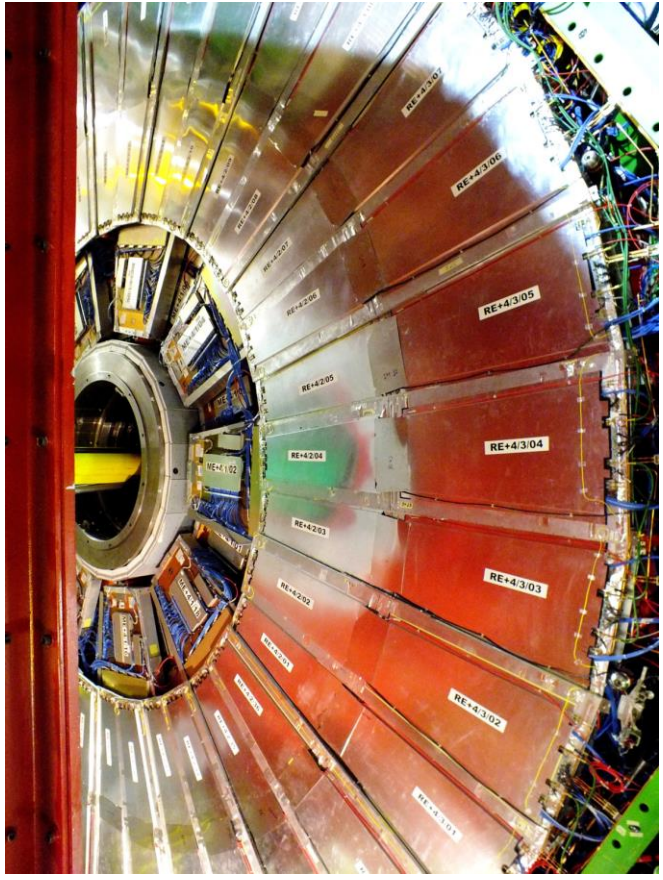

How does a Muon Spectrometer Work?

Huraaaaay again! **The same explanation as for TRT and LAr calorimeters!**

Now here's another kitty for you:

Particle Identification
(PID)

*P*article *Id*entification (PID)

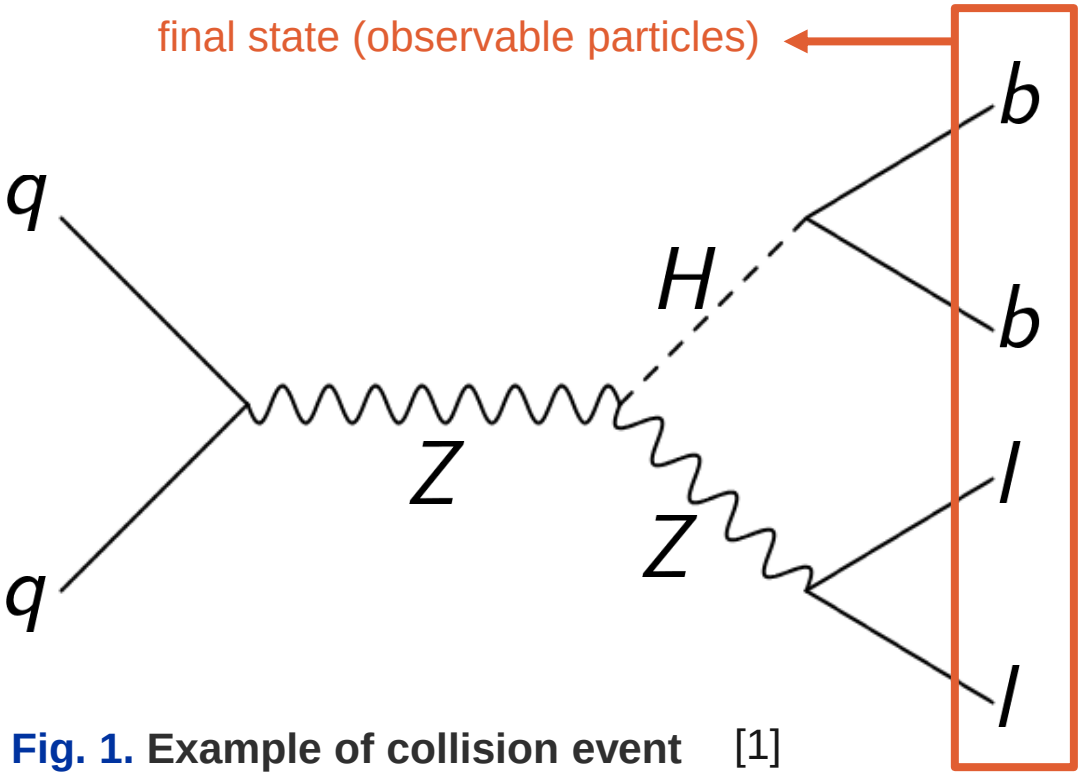

Fig. 1. Example of collision event [1]

Energy of particles is **recorded** as **hits** in the:

- trackers
- calorimeters
- muon spectrometers

Objects are **reconstructed** from the **hit information**:

- reconstruct low-level objects
- reconstruct physics objects using **tracks and clusters**, and measure **momentum**

[1] Georg VIEHHAUSER, Tony WEIDBERG; *Detectors in Particle Physics: A Modern Introduction,* 2024 (CRC Press)

Electron & Photon – Particle signatures

Fig. 2. Schematic view of e^- signature [2]

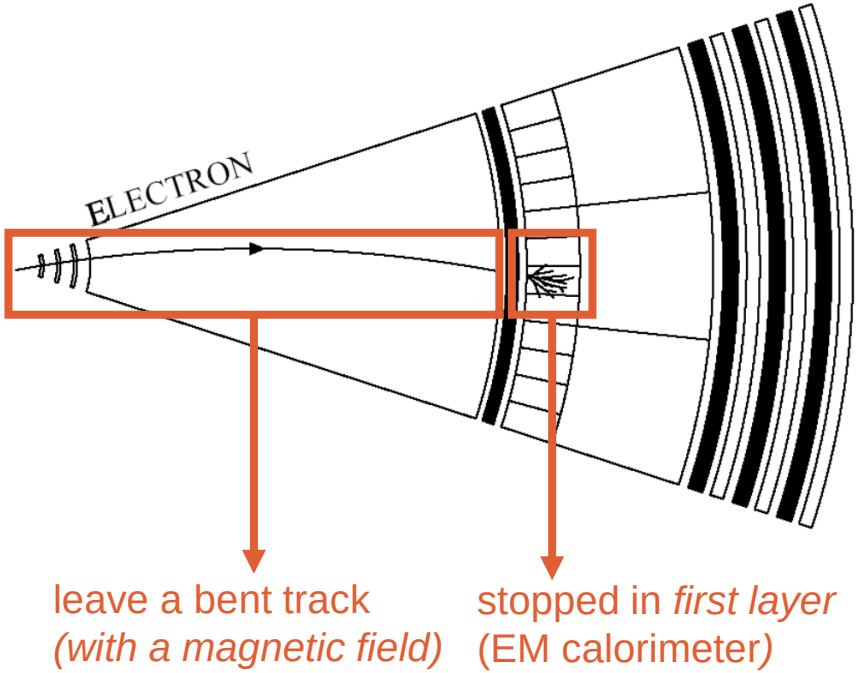

Fig. 3. Schematic view of γ signature [2]

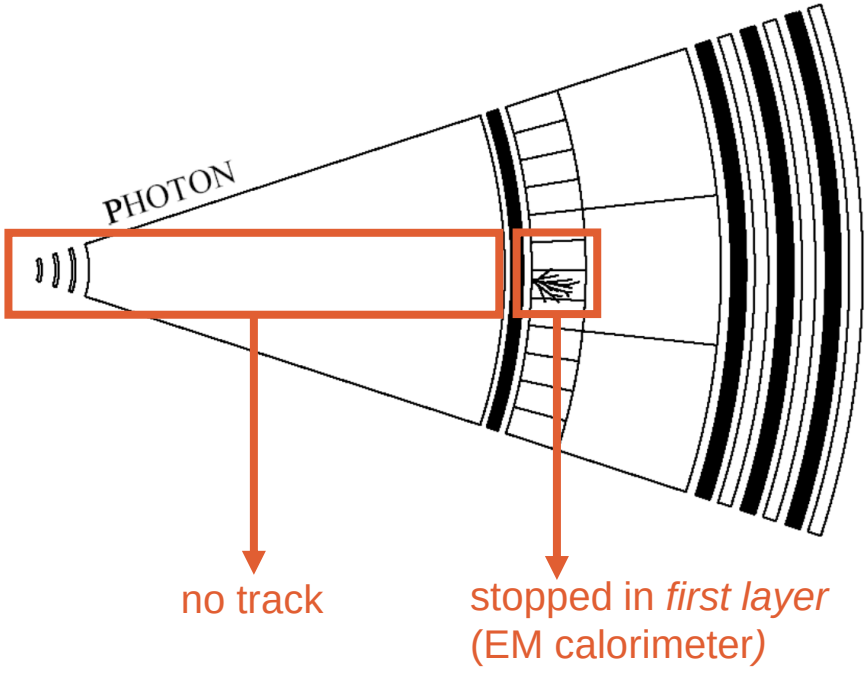

[2] Saikat BISWAS; *Particle Identification in High Energy Physics*, 2020.

Electron & Photon – Interactions with materials

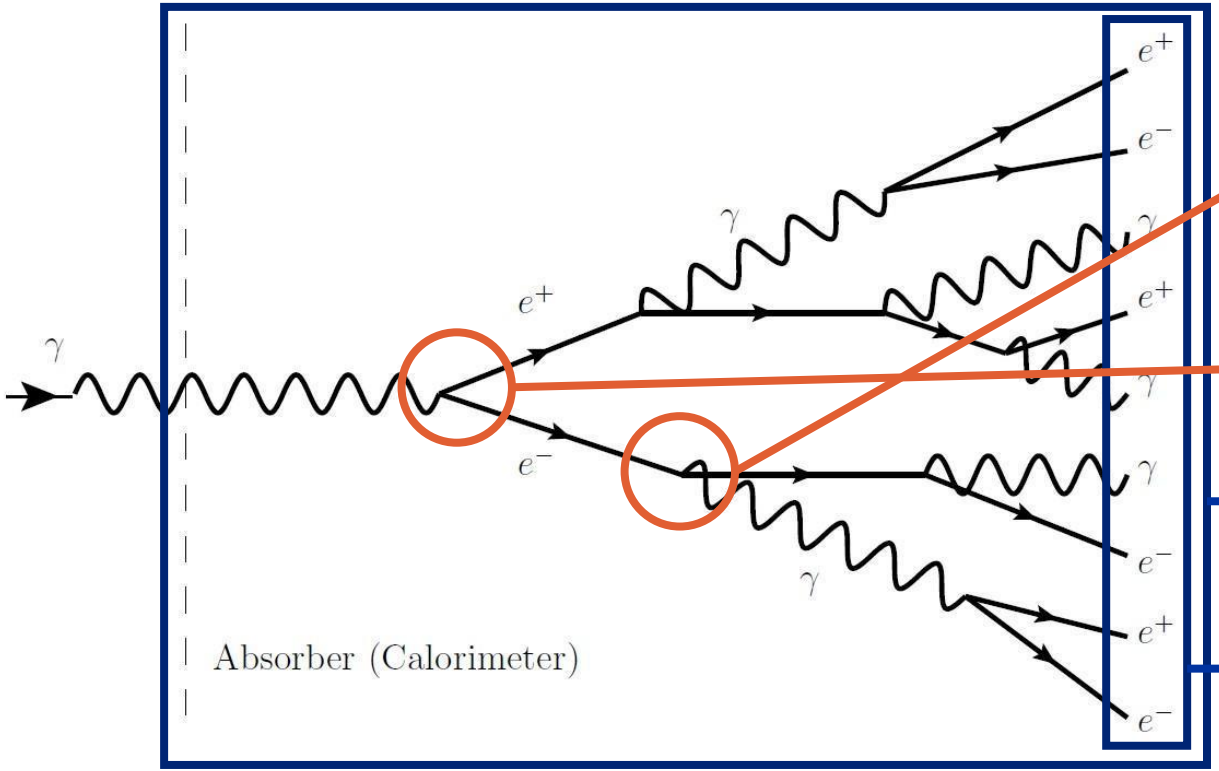

Bremsstrahlung radiation:

$$e^{\pm} + \text{materials} \rightarrow e^{\pm}\gamma$$

Pair production:

$$\gamma + \text{materials} \rightarrow e^{+}e^{-}$$

incident on matter at high energy

energy of incident particle is used up

Fig. 4. Schematic view of EM shower(photon injection) [1]

[1] Georg VIEHHAUSER, Tony WEIDBERG; *Detectors in Particle Physics: A Modern Introduction,* 2024 (CRC Press)

Electron & Photon – PID

Fig. 2'. Recap of e^- signature [2]

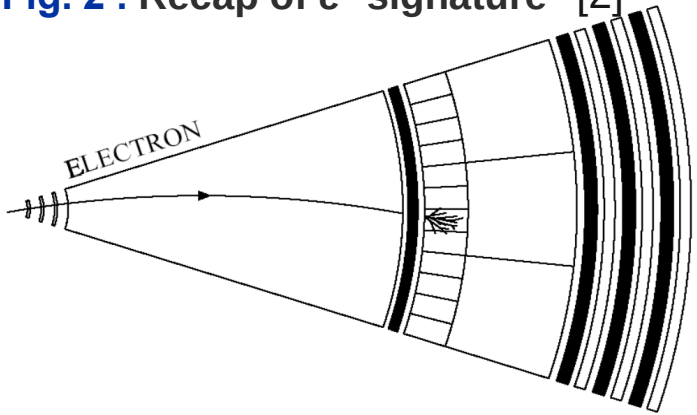

Fig. 3'. Recap of γ signature [2]

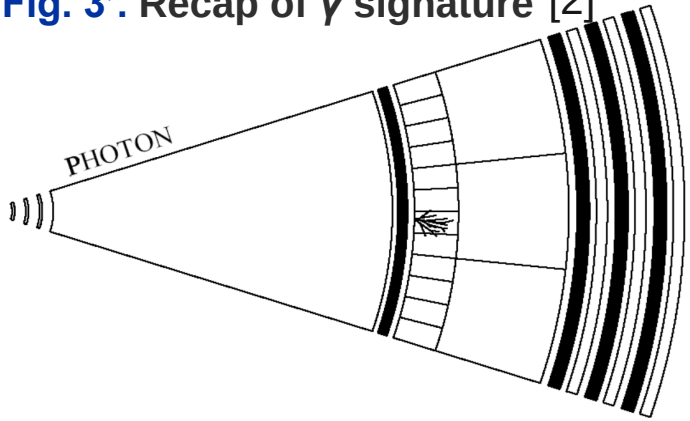

Electrons: = cluster of energy deposits in EM calorimeter + a matched track
Photons: = cluster of energy deposits in EM calorimeter + **no** matched track

If there are energy deposits in *hadronic calorimeter* (=jets), then candidates $\neq e, \gamma$

Converted photons: = identified by calorimeter cluster + *pair of opposite-charge tracks*

[2] Saikat BISWAS; *Particle Identification in High Energy Physics*, 2020.

Muon – Particle signatures

Fig. 5. Schematic view of *muon* signature [2]

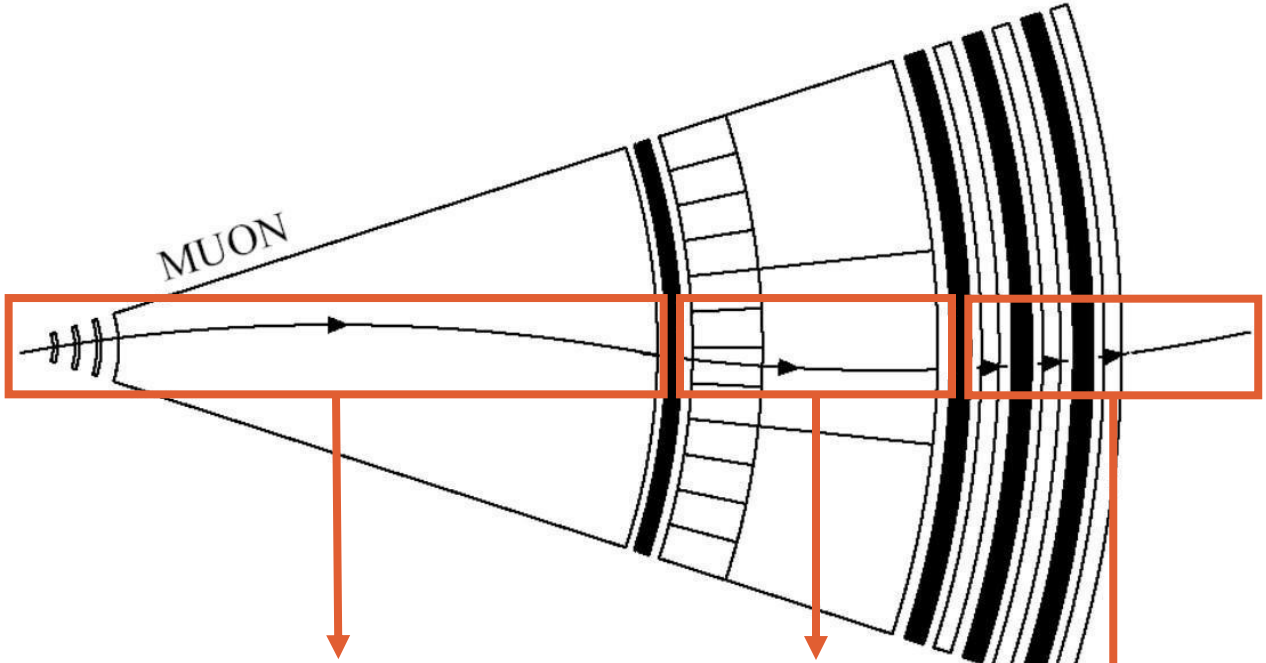

[2] Saikat BISWAS; *Particle Identification in High Energy Physics,* 2020.

Muon – PID

1. Reconstruct local tracks in ID and MS separately;

1. Combine MS and ID tracks;

1. Global fit based on ID & MS hits, taking into account energy loss in the calorimeters;

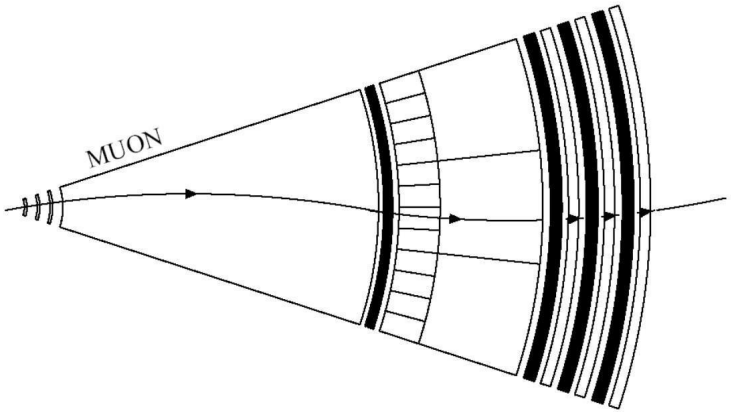

Fig. 5'. Recap of *muon* signature [2]

[3]

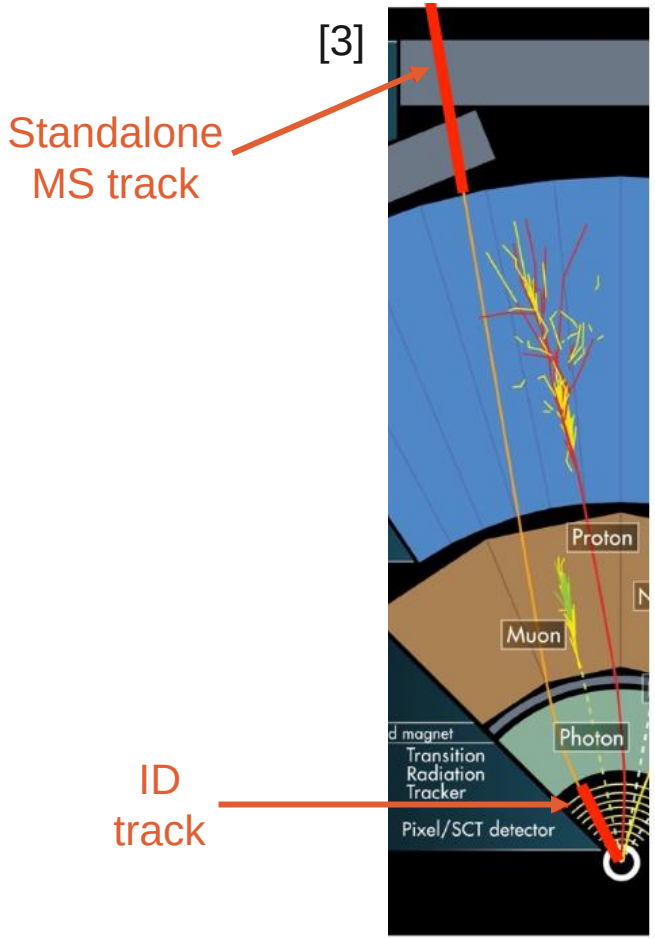

[3] Roger FORTY; *Particle Identification (CERN);* ICFA Instrumentation School, 1-2 December 2017

Muon – PID: reconstruction efficiencies

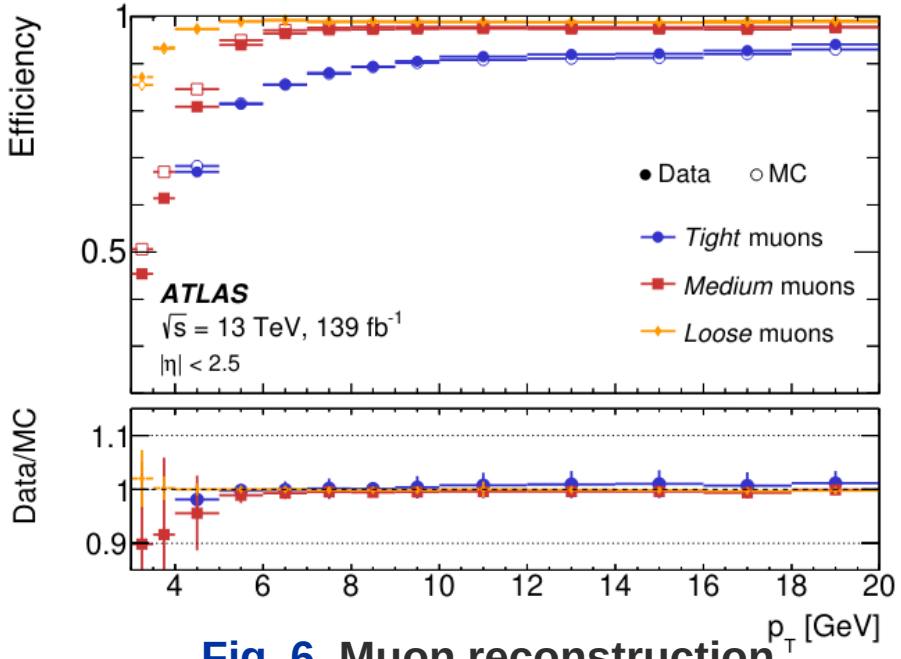

Fig. 6. Muon reconstruction efficiencies for events $J/\psi \rightarrow \mu\mu$ [4]

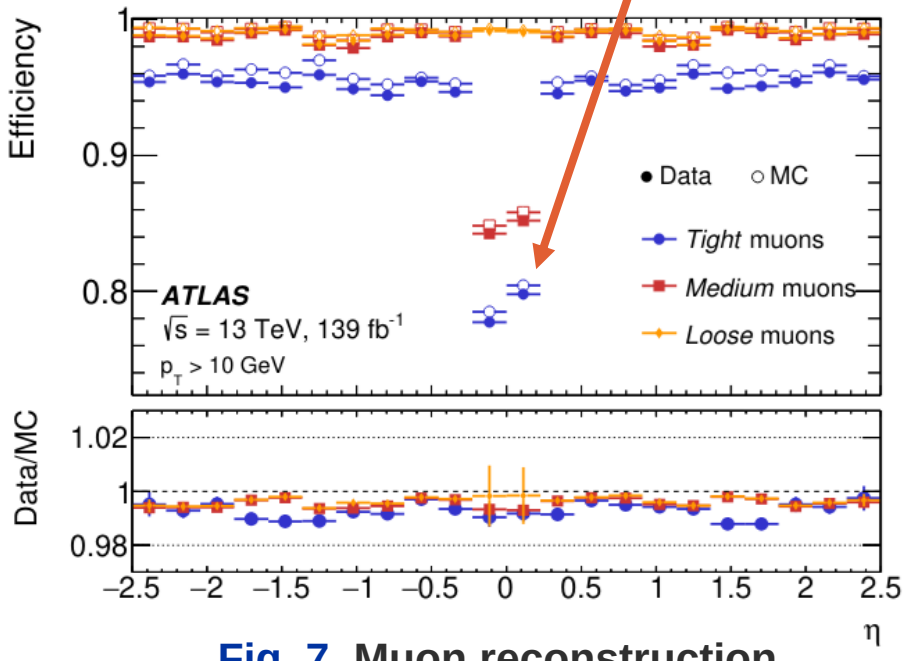

Fig. 7. Muon reconstruction efficiencies for events $Z \rightarrow \mu\mu$ [4]

[4] The ATLAS Collaboration, CERN; *Muon reconstruction and identification efficiency in ATLAS using the full Run 2 pp collision data set at √s = 13 TeV,* Eur. Phys. J. C 81 (2021) 578

Hadron – Particle signatures

Fig. 8. View of *charged hadron* signature [2]

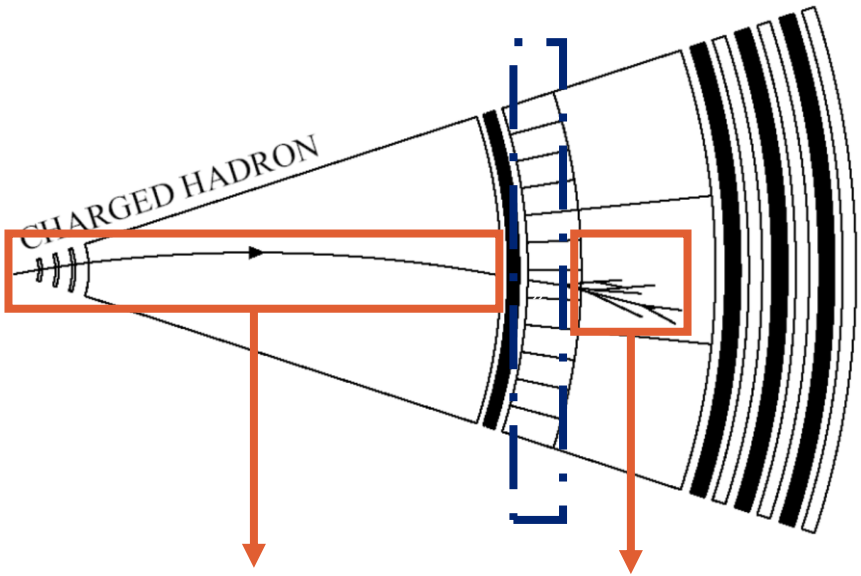

leave a bent track
(with a magnetic field)

stopped deep in
second layer
(hadronic calorimeter)

Fig. 9. View of *neutral hadron* signature [2]

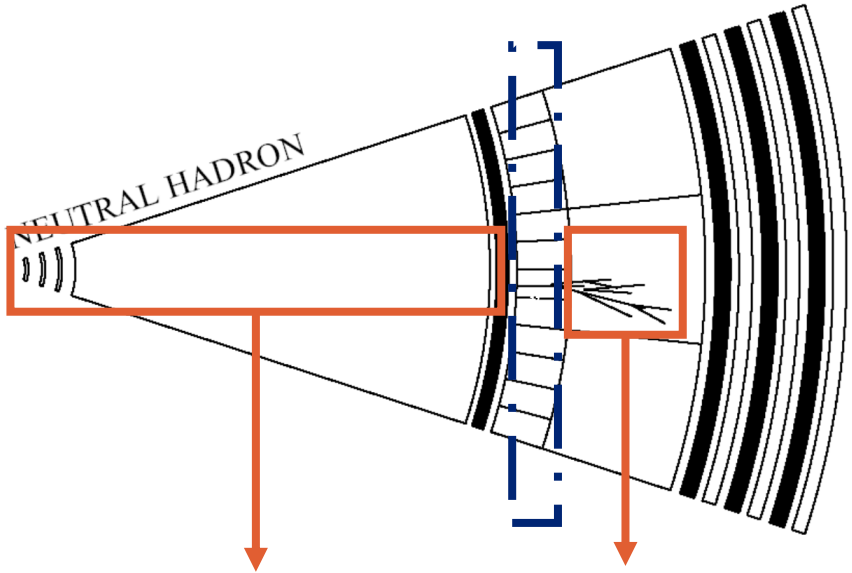

no track

stopped deep in
second layer
(hadronic calorimeter)

[2] Saikat BISWAS; *Particle Identification in High Energy Physics*, 2020.

Hadron – Interactions with materials

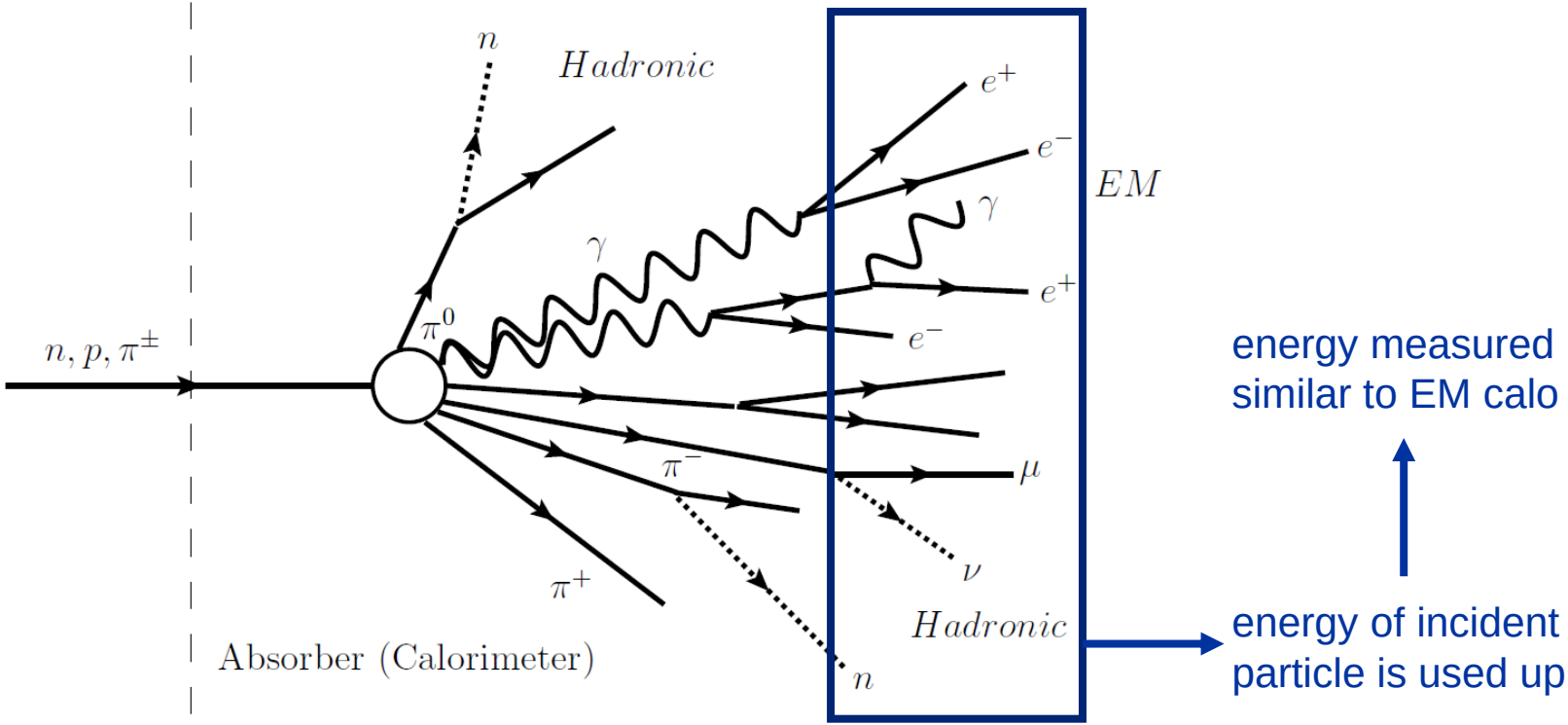

Fig. 10. Schematic view of hadronic shower (hadron injection) [1]

[1] Georg VIEHHAUSER, Tony WEIDBERG; *Detectors in Particle Physics: A Modern Introduction,* 2024 (CRC Press)

Neutrino – Missing Transverse Energy (MET)

Neutrinos don’t interact with detectors $\longrightarrow$ Missing Transverse Energy: E_T^{miss}

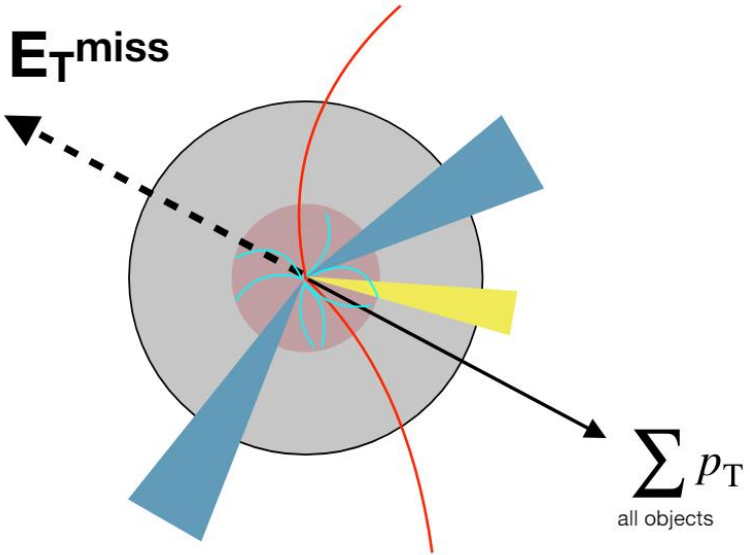

Fig. 11. Transversal section of detector [5]

Conservation of momentum:

$$\sum \vec{p}_T^{\,\text{visible}} + \sum \vec{p}_T^{\,\text{invisible}} = \vec{0}$$

Missing E_T^{miss}

Reconstruct the visible objects:

$$\vec{p}_T^{\,miss} = -\sum_{\text{all objects}} \vec{p} \quad \rightarrow E_T^{miss}$$

[5] The ATLAS Collaboration, CERN; *Performance of missing transverse momentum reconstruction with the ATLAS detector using proton-proton collisions at √s = 13 TeV, Eur. Phys. J. C 78 (2018) 903.*

PID methods – Mass determination

Relativistic momentum: $\vec{p} = \gamma m_0 \vec{v}$

$$\vec{\beta} = \frac{\vec{v}}{c} \qquad \gamma = \frac{1}{\sqrt{1-\beta^2}}$$

Rest mass: $m_0 = \frac{p}{c\beta\gamma}$

momentum can be measured thanks to the magnetic field *[charged particle]*

Lorentz variables can be determined:

- *Time-of-flight (TOF)*
- *Energy loss by ionisation (dE/dx)*
- *Cherenkov radiation*
- *Transition radiation*

[6] Edwin F. TAYLOR, John Archibald WHEELER; *Spacetime Physics: Introduction to Special Relativity.* 1992, W. H. Freeman.

PID methods – Time-of-flight (TOF) measurements

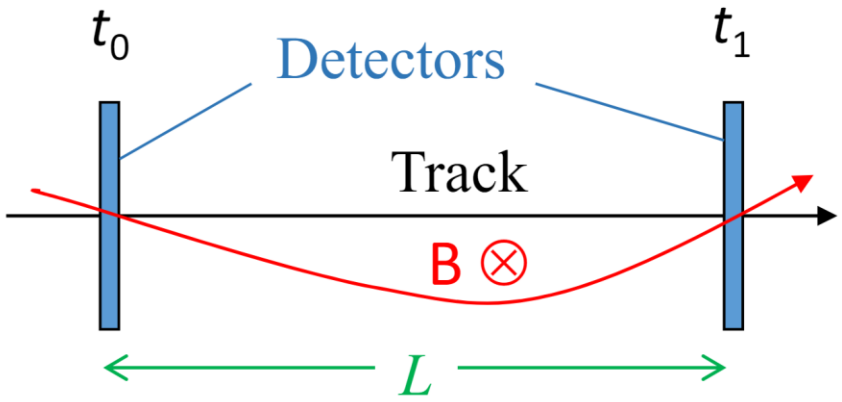

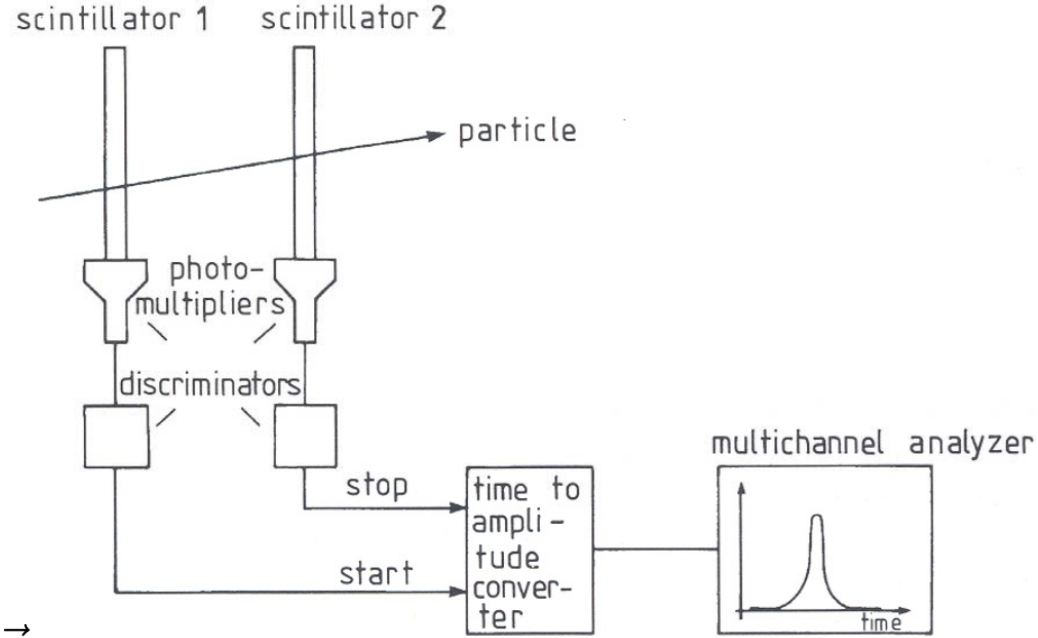

Difference in arrival time: $\beta = \frac{L}{ct}$

Relativistic momentum: $\vec{p} = \gamma m_0 \vec{v}$

Calculated mass: $m^2_{\mathrm{TOF}} = \frac{p^2}{c^2}\left(\frac{c^2 t^2}{L^2} - 1\right)$

Fig. 12. Typical TOF set-up (diagram & specific) [7]

[7] Roger FORTY; *Time-of-flight technologies (CERN);* ECFA R&D Roadmap Symposium, 6 May 2021.

TOF – Flight-time plots for different particles

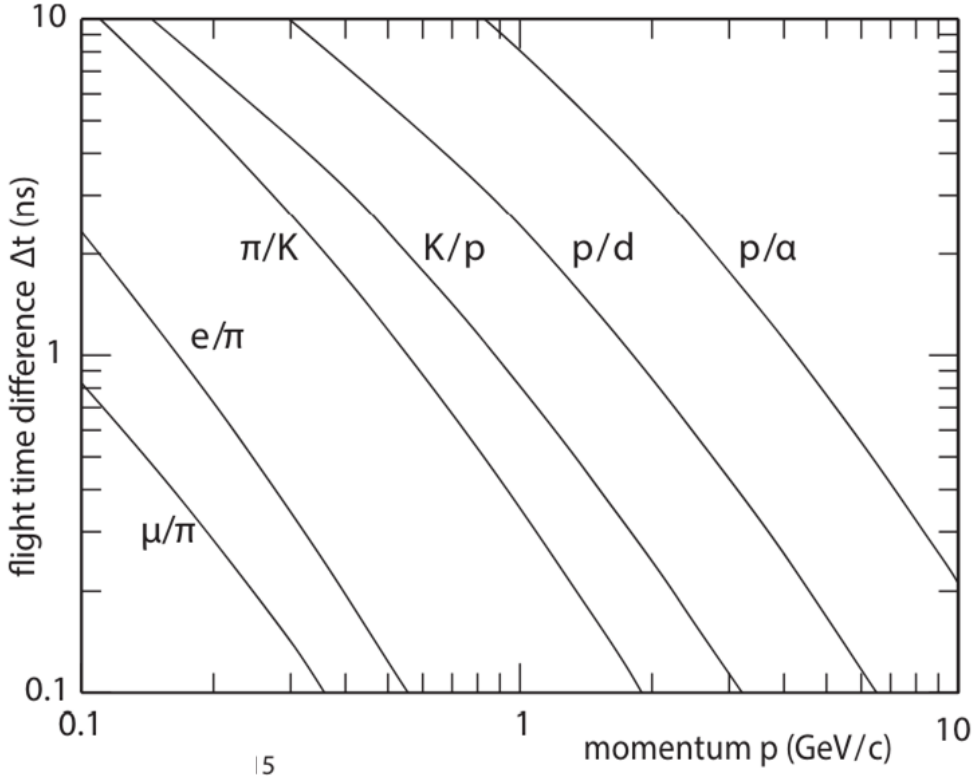

Flight-time: $$t_{\mathrm{TOF}} = \frac{L}{c}\sqrt{\frac{p^2 + m^2c^2}{p^2}}$$

Difference in flight-times:

$$\frac{t_{\mathrm{TOF},2} - t_{\mathrm{TOF},1}}{L} \approx \frac{1}{2cp^2}(m_2^2 - m_1^2)c^2$$

Relativistic approximation:

$$p^2 \gg m^2c^2$$

Fig. 13. TOF differences for pairs of pairs of particles at flight distance *L = 1 m.* [8]

[8] Hermann KOLANOSKI, Norbert WERMES; *Particle Detectors,* 2022 (ed princeps 2020), Oxford University Press.

TOF – Separation of *π,K,p* (Mark III experiment, SLAC)

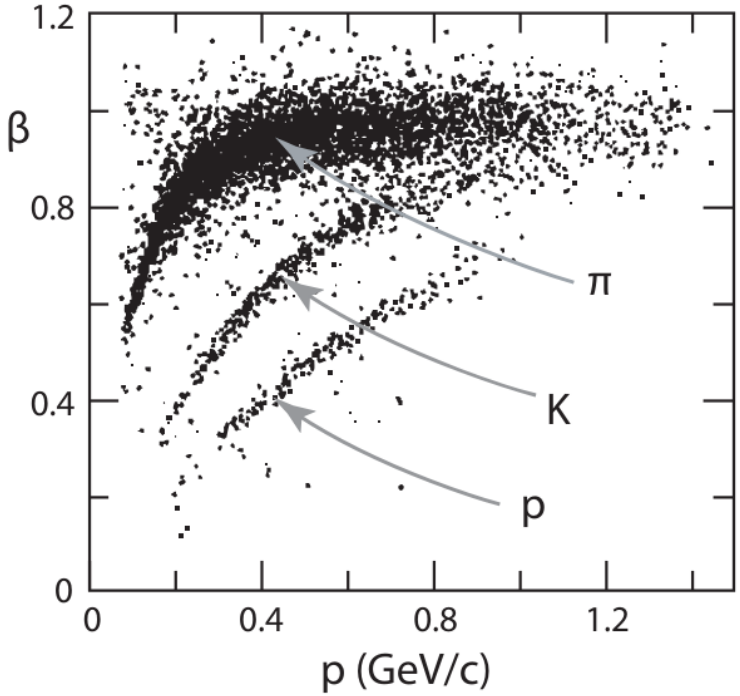

(a) β–p plot.

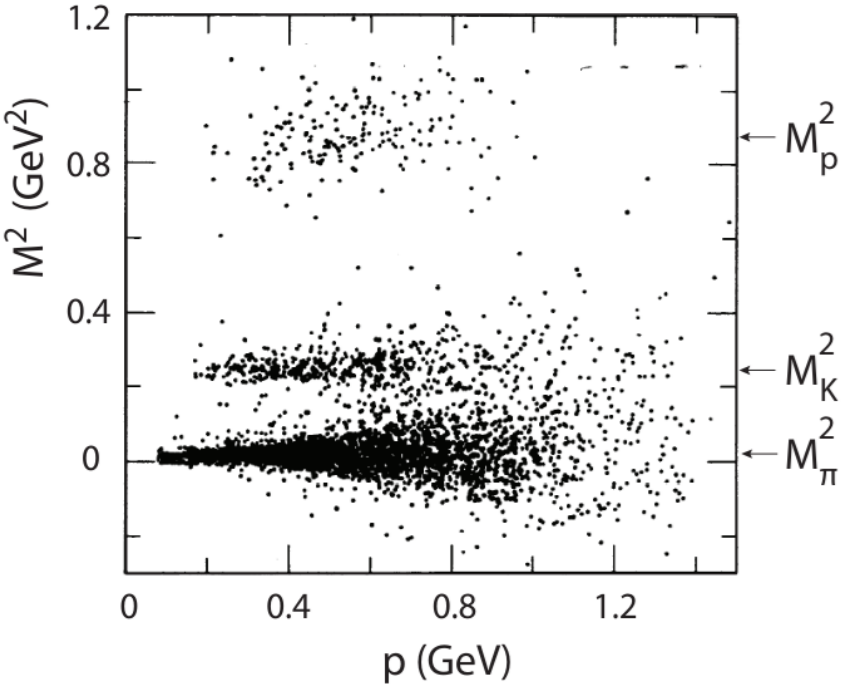

(b) TOF squared mass.

Fig. 14. Type separation w.r.t particle velocity [8]

Fig. 15. Separation using TOF mass [8]

[8] Hermann KOLANOSKI, Norbert WERMES; *Particle Detectors,* 2022 (ed princeps 2020), Oxford University Press.

PID methods – Energy deposit by ionisation

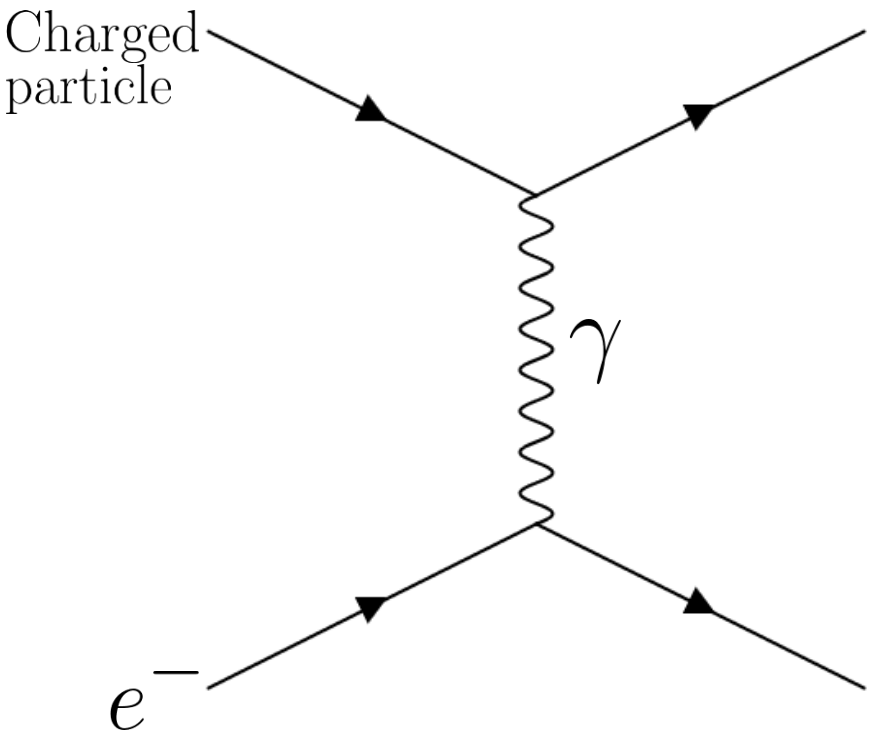

Fig. 16. Diagram of energy deposit by ionisation [1']

[1] Georg VIEHHAUSER, Tony WEIDBERG; *Detectors in Particle Physics: A Modern Introduction,* 2024 (CRC Press)

Ionisation – Bethe-Bloch formula for heavy particles

Energy loss for heavy charged particles: $Mc^2 \gg m_e c^2$

$0.1 \lesssim \beta\gamma \lesssim 1000$
$\text{intermediate} - Z \text{ materials}$

Interaction dominated by elastic collisions with electrons

high E low E $\beta c \sim v_e$

$$-\left\langle \frac{dE}{dx} \right\rangle = Kz^2 \frac{Z}{A}\frac{1}{\beta^2}\left[\frac{1}{2}\ln\frac{2m_e c^2\beta^2\gamma^2 T_{max}}{I^2} - \beta^2 - \frac{\delta(\beta\gamma)}{2} - \frac{U(\beta\gamma)}{2}\right]$$

maximum energy transfer in single collision

mean excitation energy of medium

density-effect correction *[transverse extension of electric field]*

shell-effect correction *[correct neglection of atomic binding]*

Non-relativistic region $(\beta\gamma < 4)$: $-\left\langle \frac{dE}{dx} \right\rangle_{\text{classical}} \propto \frac{1}{\beta^2}\ln(\text{const}\cdot\beta^2\gamma^2)$

[9] Particle Data Group PDG 2010; *27. Passage of particles through matter*; Revised January 2010 by H. Bichsel (University of Washington), D.E. Groom (LBNL), and S.R. Klein (LBNL).

Ionisation – Stopping power w.r.t. parameter *βγ* (1)

saturation at large *(βγ)* due to density-effect (correction *δ*) *[polarization of medium]*

$dE/dx \propto \ln(\beta\gamma)^2$

[relative extension of transversal electric field]

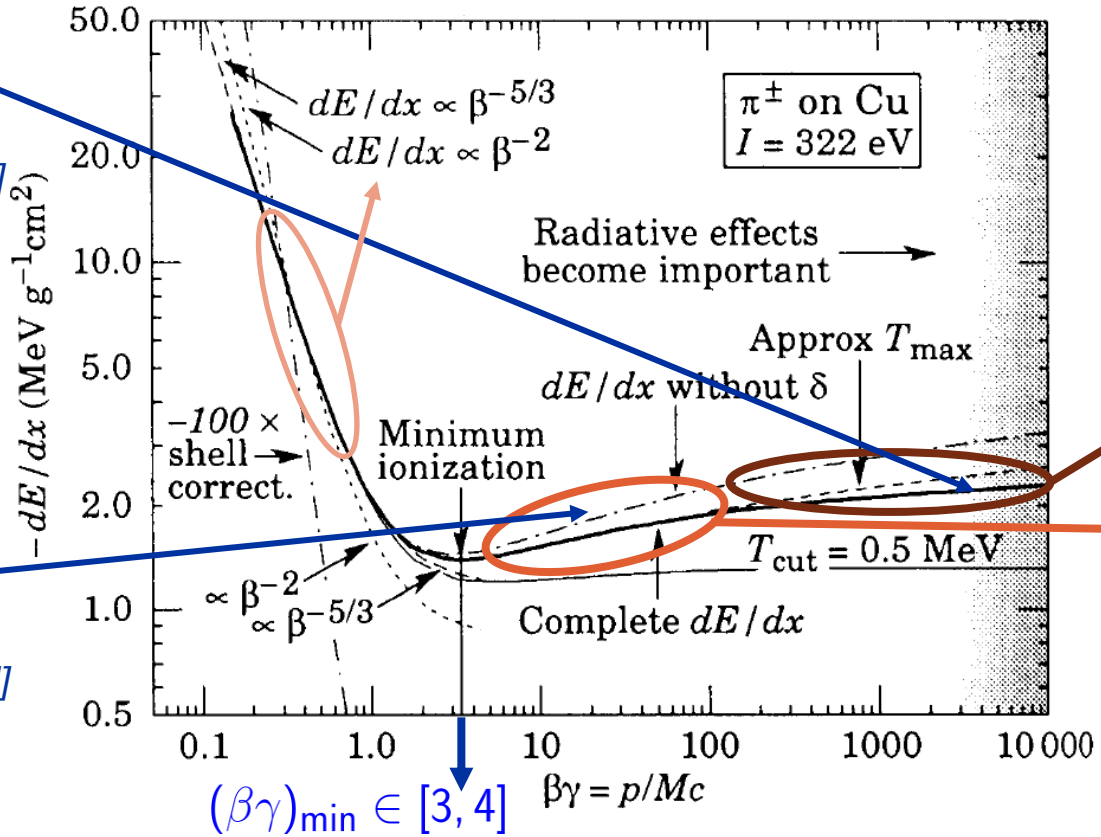

$(\beta\gamma)_{min} \in [3, 4]$

Fermi plateau

log rise

Fig. 17.
Stopping power development
(log-log graph)
[9]

[9] Particle Data Group PDG 2010; *27. Passage of particles through matter*; Revised January 2010 by H. Bichsel (University of Washington), D.E. Groom (LBNL), and S.R. Klein (LBNL).

Ionisation – Minimum ionization for materials

$$-\left\langle \frac{dE}{dx} \right\rangle_{\text{min}} \sim \frac{Z}{A}$$

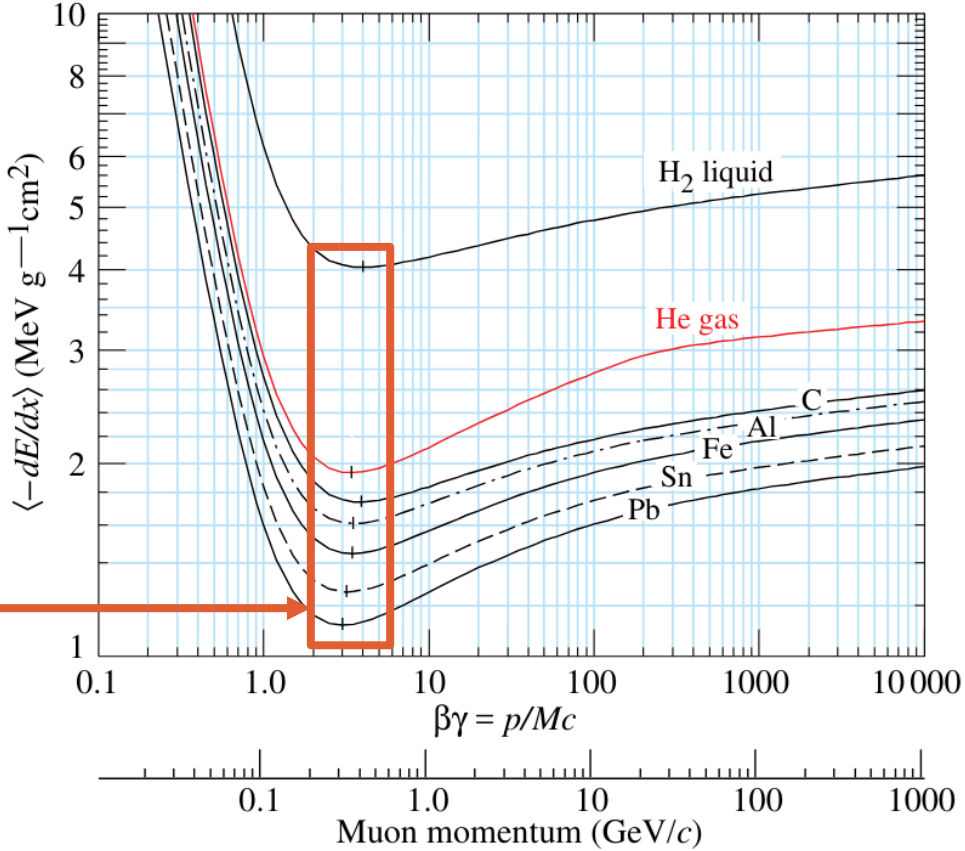

Fig. 18. Behaviour of stopping power for different materials [10]

[10] Particle Data Group PDG 2019; *33. Passage of particles through matter*; Revised August 2019 by D.E. Groom (LBNL) and S.R. Klein (NSD LBNL).

Ionisation – Bethe-Bloch formula for electrons

Incident and target electrons have the same mass: $M = m_e$

scattering of identical, indistinguishable particles

$$-\left\langle \frac{\mathrm{d}E}{\mathrm{d}x} \right\rangle_{\mathrm{el}} = K \frac{Z}{A} \frac{1}{\beta^2} \left[\ln \frac{m_e \beta^2 c^2 \gamma^2 T}{2I^2} + F(\gamma) \right]$$

mean excitation energy of medium

kinetic energy of electron

independent term univariately dependent on Lorentz factor

Positrons are not identical with electrons, i.e. different treatment!

[9] Particle Data Group PDG 2010; *27. Passage of particles through matter*; Revised January 2010 by H. Bichsel (University of Washington), D.E. Groom (LBNL), and S.R. Klein (LBNL).

Ionisation – Identification: *specific ionization* plots

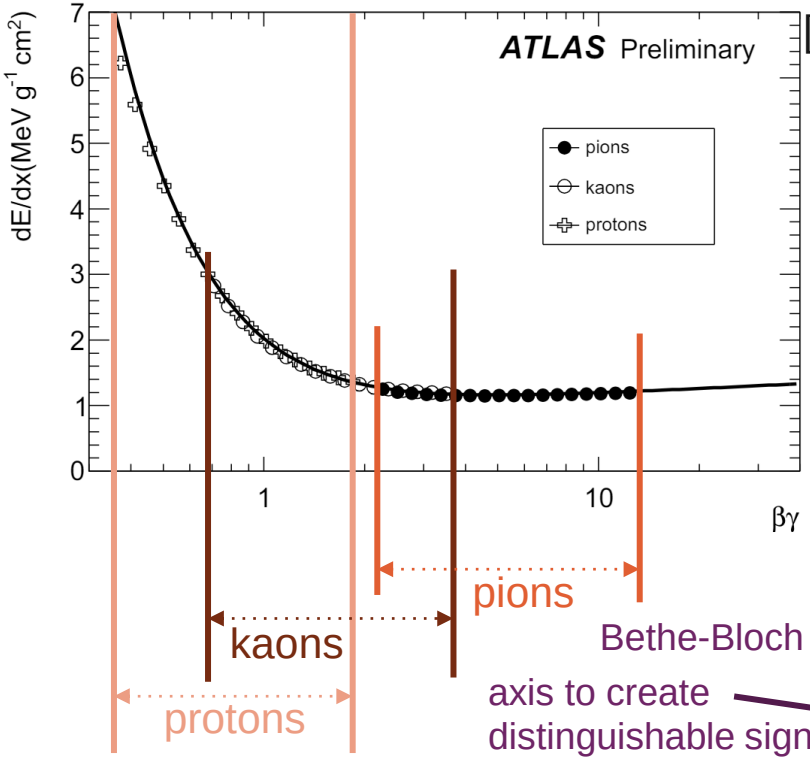

[11]

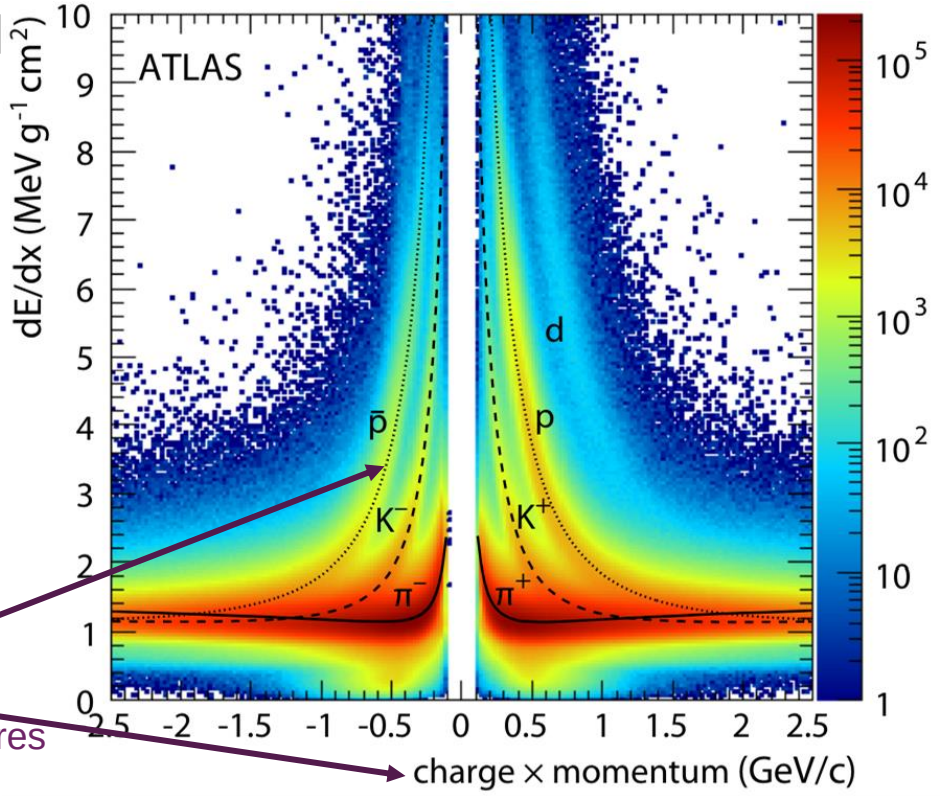

[11]

Fig. 19. Distribution of MPV$_{dE/dx}$ with parametric expression derived from MC simulated tracks

Fig. 20. Charged, low momentum particle ID (ATLAS)

[11] G. AAD, et al.; *Searches for heavy long-lived sleptons and R-hadrons with the ATLAS detector in pp collisions at √s = 7 TeV.* In: Phys. Lett. B 720 (2013)

PID methods – Detection of Cherenkov radiation

Occurs when a charged particle traverses a medium in which its velocity is greater than the phase velocity of light in that medium: $v > c_n = c/n$, emitting electromagnetic radiation.

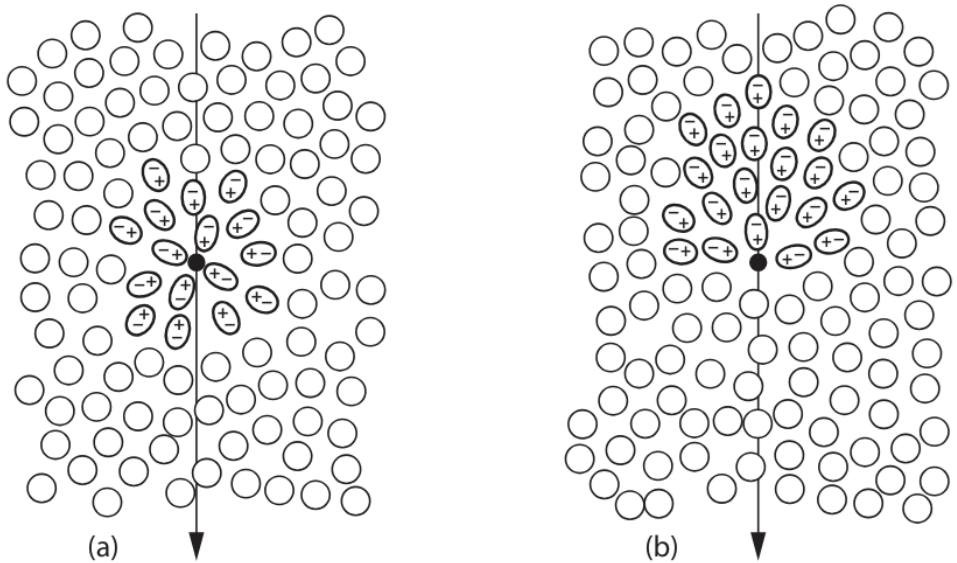

Fig. 21. Cherenkov radiation, as caused by an asymmetry in the polarisation of the dielectric medium [8]

[8] Hermann KOLANOSKI, Norbert WERMES; *Particle Detectors,* 2022 (ed princeps 2020), Oxford University Press.

Cherenkov radiation – General characteristics

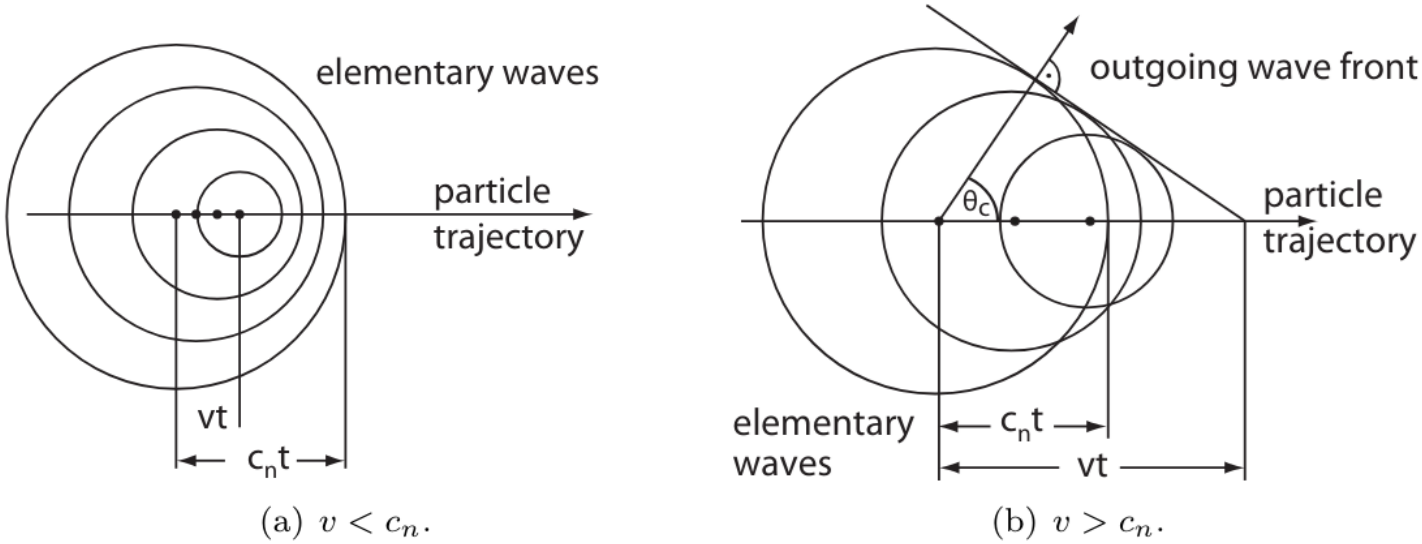

Fig. 22. Geometry of the outgoing wave front for Cherenkov radiation [8]

Cherenkov angle: $\cos\theta_c = \frac{c_n t}{vt} = \frac{1}{\beta n}$ $\theta_c = \arccos\frac{1}{\beta n}$ $n = \sqrt{\epsilon_r \mu_r}$

[8] Hermann KOLANOSKI, Norbert WERMES; *Particle Detectors,* 2022 (ed princeps 2020), Oxford University Press.

Cherenkov radiation – Mass calculation

Relativistic momentum: $\vec{p} = \gamma m_0 \vec{v} = \vec{\beta}\gamma m_0 c$

Mass calculation: $m_0^2 = \frac{p^2}{c^2}\left(\frac{1}{\beta^2} - 1\right)$

Remember: $\cos\theta_c = \frac{1}{\beta n}$

Mass calculation using Cherenkov angle: $m_0^2 = \frac{p^2}{c^2}\left(n^2\cos^2\theta_c - 1\right)$

Cherenkov radiation – Identification: *angle* (ALICE)

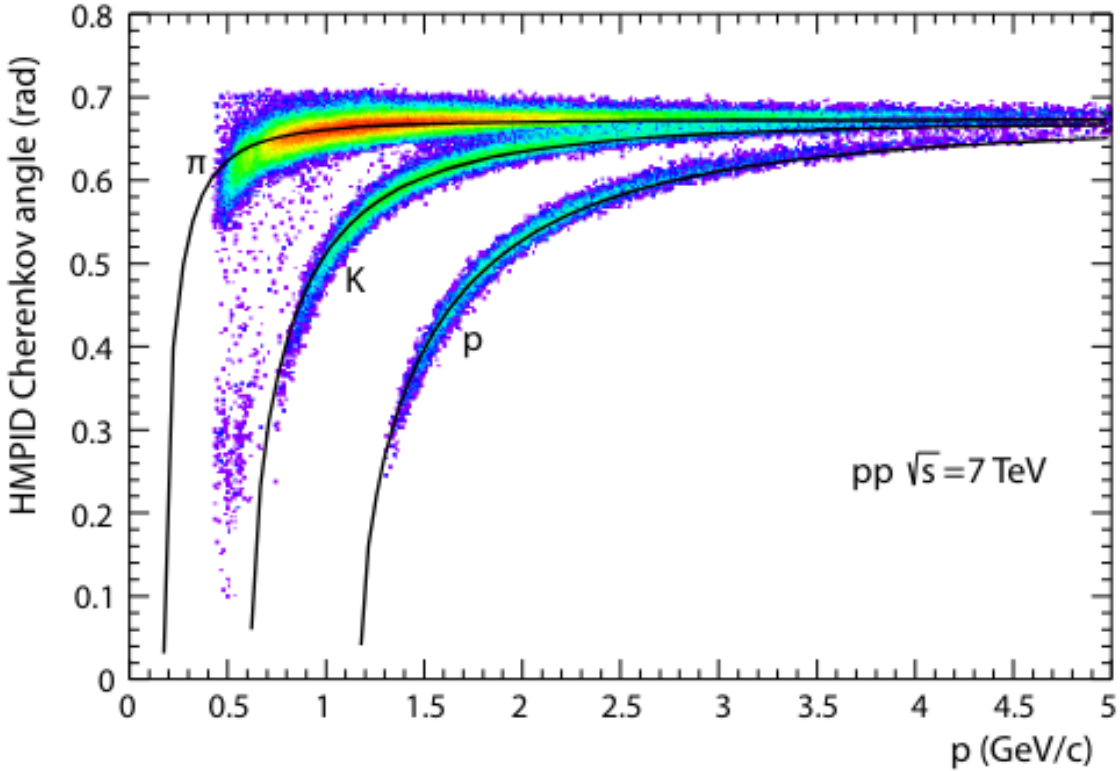

Fig. 23. Cherenkov angle w.r.t. momentum create distinct plots [8]

[8] Hermann KOLANOSKI, Norbert WERMES; *Particle Detectors,* 2022 (ed princeps 2020), Oxford University Press.

PID methods – Detection of Transition radiation

Occurs when a relativistic particle $(\beta \to 1)$ traverses the boundary between two media with different electric permittivities $(\epsilon_1 \neq \epsilon_2)$, emitting photons with energies up to the high-energy X-ray regime.

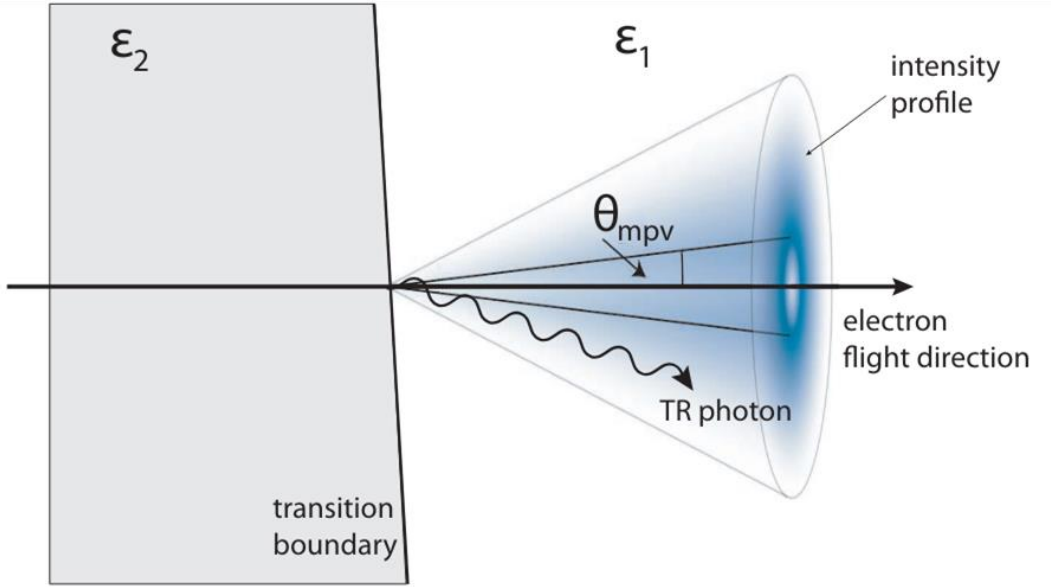

Fig. 24.
Transition radiation and possible angles TR photons can take [8]

[8] Hermann KOLANOSKI, Norbert WERMES; *Particle Detectors,* 2022 (ed princeps 2020), Oxford University Press.

Transition radiation – General characteristics

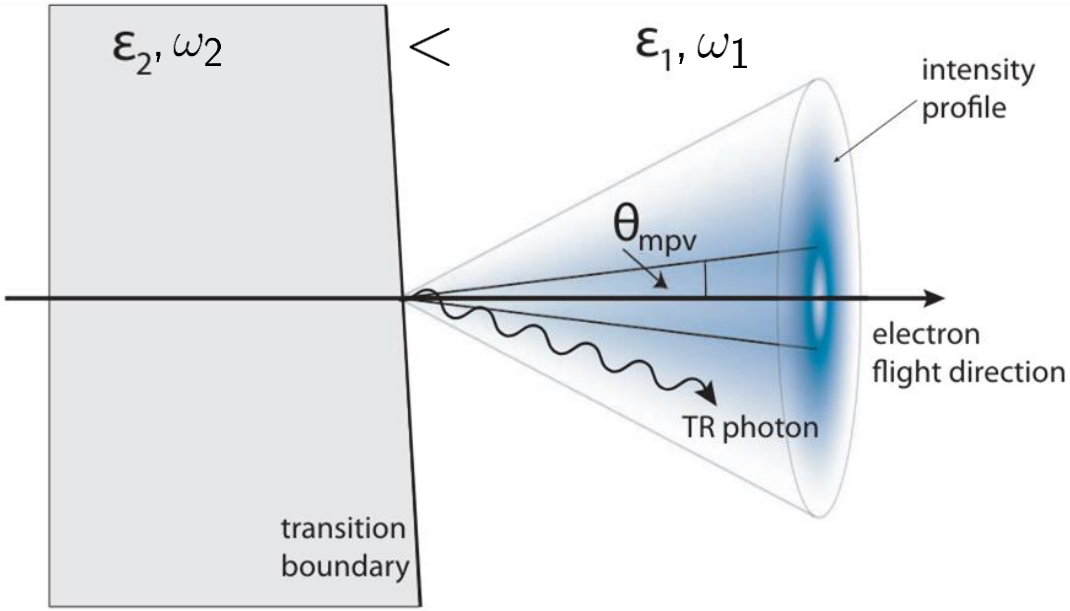

Intensity: $I_{TR} \propto \gamma$

Emission angle: $\theta_{mpv} \propto \frac{1}{\gamma}$

Emission energy: $E_{TR} \propto (\epsilon_2 - \epsilon_1)$

- low photon emission probability per transition
- gas with high photon absorption *(high Z)* required

Fig. 24'. Recap of TR radiation geometry [8] [12]

[12] Marco DELMASTRO, *3. Particle interactions in particle detectors*, European School of Instrumentation in Particle & Astroparticle Physics

Transition radiation – High threshold hit fraction

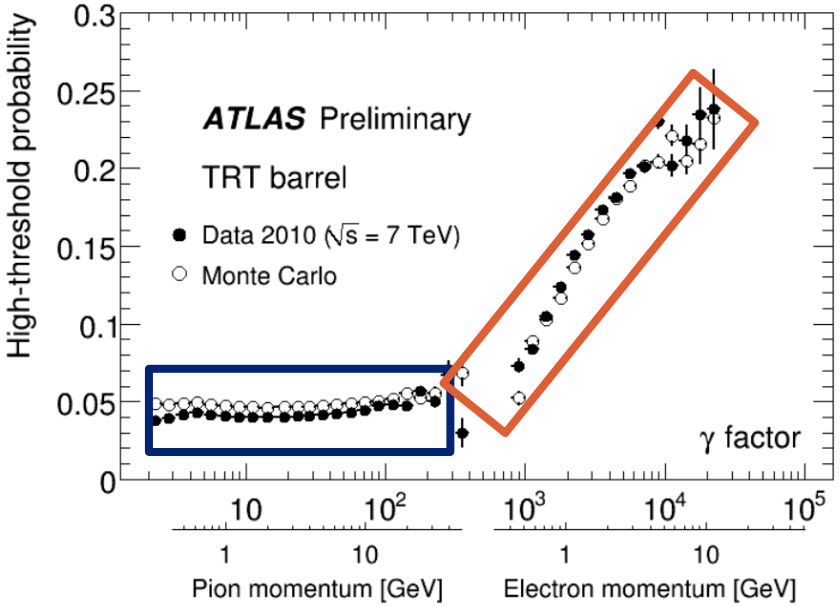

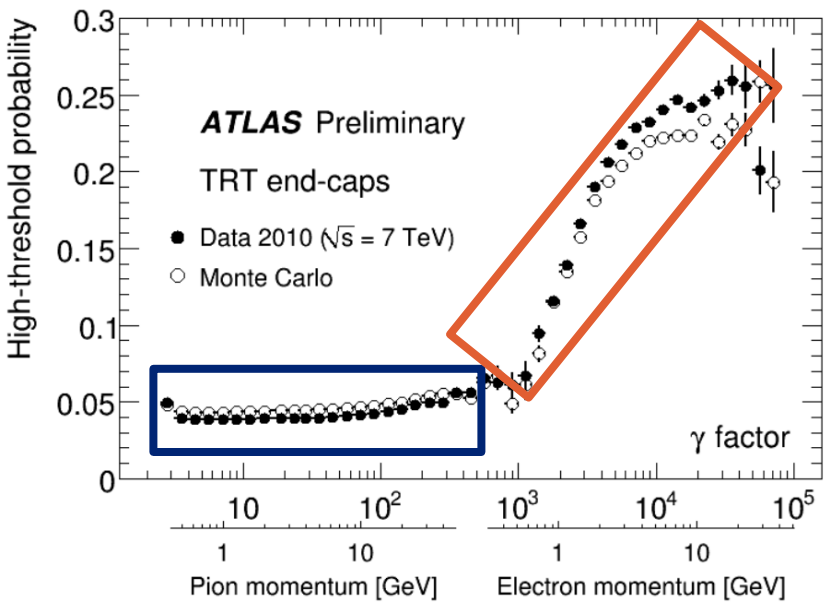

Fig. 25 & 26. TRT High Threshold hit fraction defined by: $p = \frac{[\text{HT hits on tracks}]}{[\text{LT hits on tracks}]}$ provides electron/hadron discrimination *over the momentum range between [1,150] GeV/c* [13]

[13] Ahmet BINGUL (On behalf of ATLAS TRT Collaboration); *The ATLAS TRT and its Performance art LHC,* ICPP-II, 2011

Transition radiation – Identification: *fraction of hits*

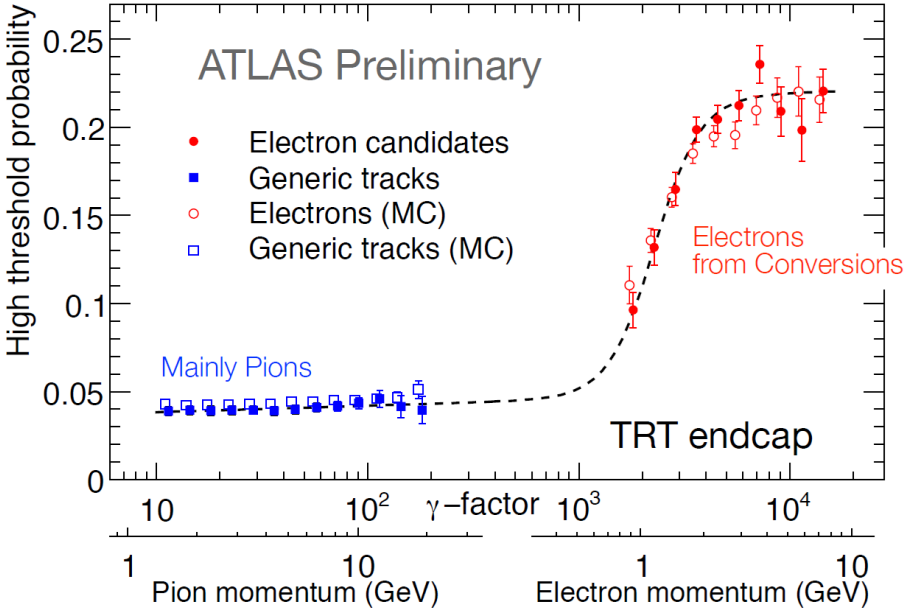

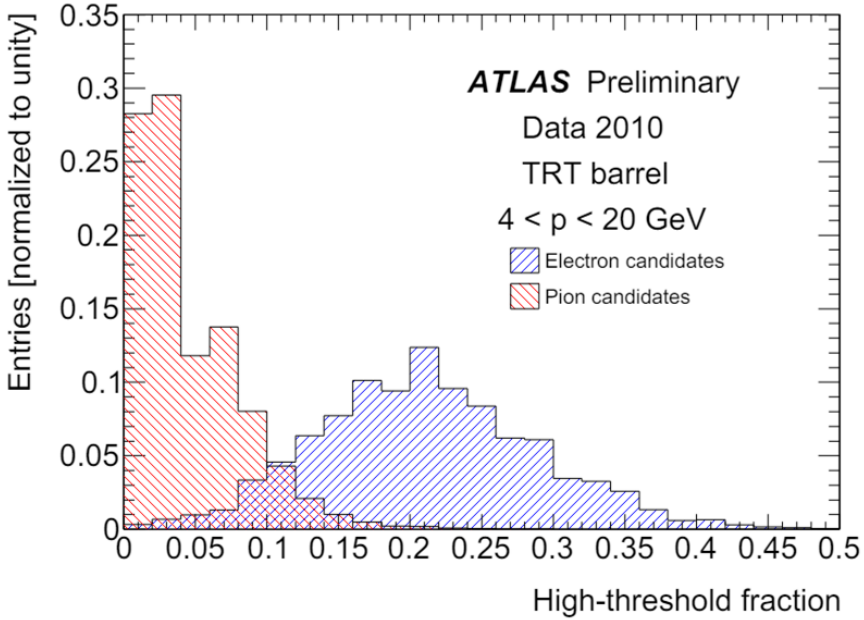

Fig. 27. Phase spaces for particle types

Fig. 28. High-threshold fraction distribution [12]

[12] Marco DELMASTRO, *3. Particle interactions in particle detectors*, European School of Instrumentation in Particle & Astroparticle Physics

Particle reconstruction – V^0s (example)

K_S^0 and Λ are collectively known as V^0s, due to their characteristic two-prong decay vertex:

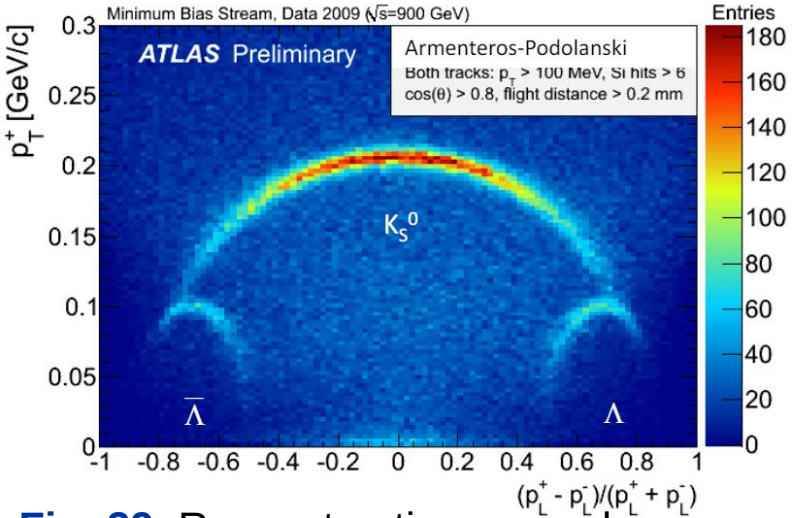

Fig. 29. Reconstruction example

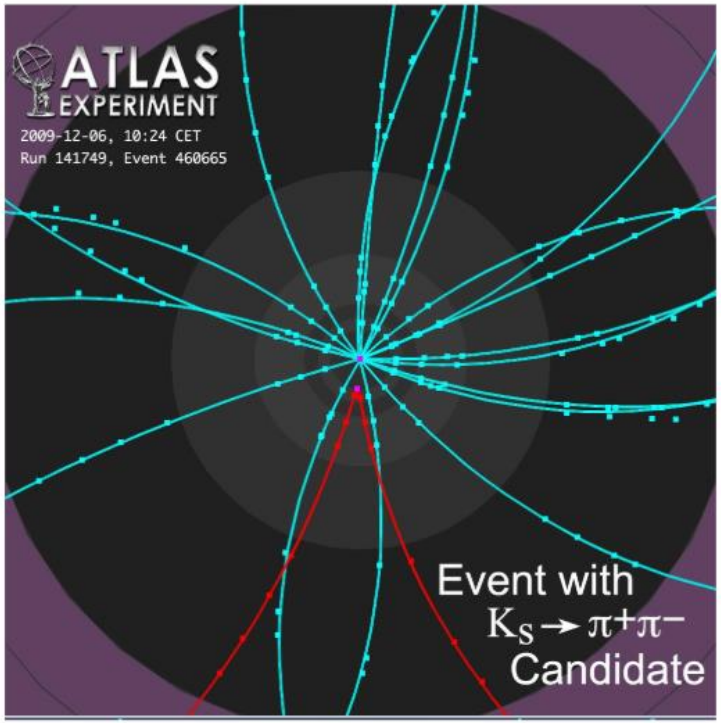

Fig. 30. Decay of V^0s [2]

[2] Saikat BISWAS; *Particle Identification in High Energy Physics*, 2020.

Mass reconstruction – Higgs boson

Fig. 31. Mass reconstruction for pion $\pi^0 \rightarrow \gamma\gamma$

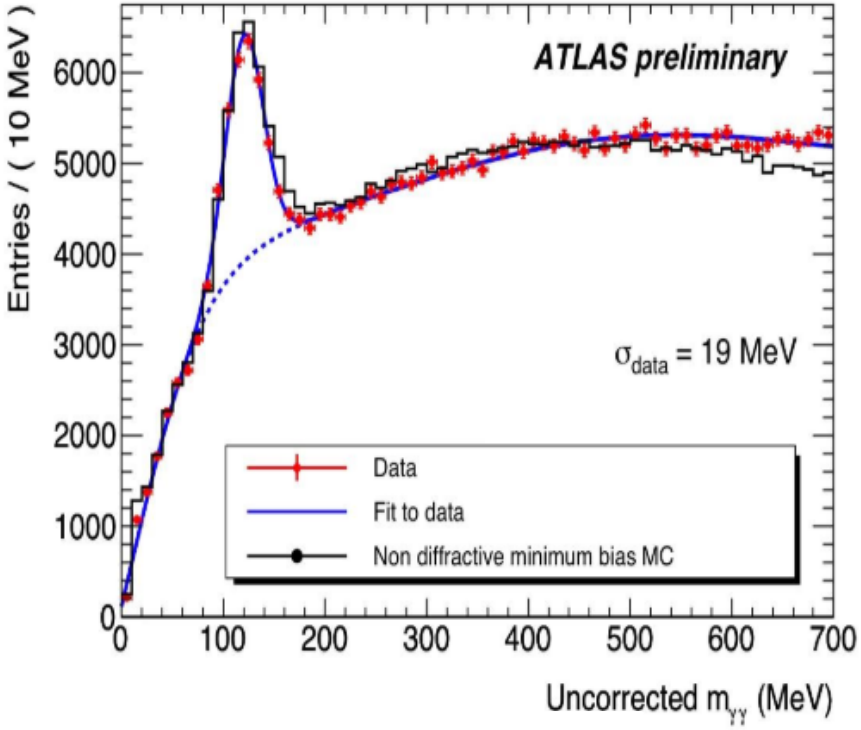

Fig. 32. Mass reconstruction for Higgs $H \rightarrow \gamma\gamma$

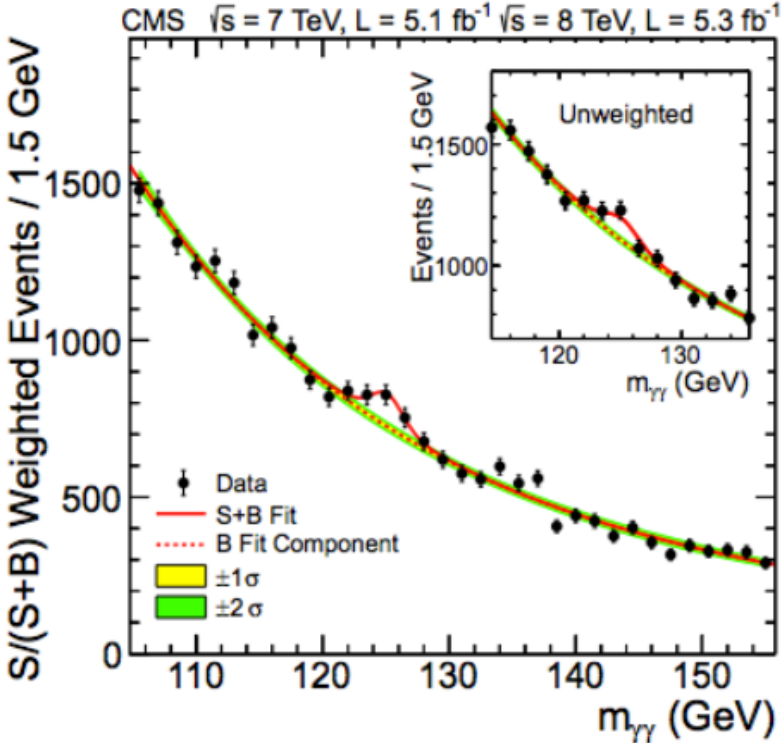

Bibliography

-[1] ATLAS Pixel Collaboration, ATLAS Pixel Detector Technical Design Report, CERN/LHCC/98-13 (1998).

-[2] ATLAS Collaboration, ATLAS TDR-5, CERN/LHCC/97-17 (1997).

-[3] ATLAS Inner Detector Volume I Technical Design Report

-[4] The ATLAS Experiment at the CERN Large Hadron Collider, PUBLISHED BY INSTITUTE OF PHYSICS PUBLISHING AND SISSA

-[5] ATLAS Experiment at CERN

-[1]-[13](P) All references and citations are given at the footer of each slide in detail. Consult references there!